

CZECH TECHNICAL UNIVERSITY IN PRAGUE

FACULTY OF CIVIL ENGINEERING

DEPARTMENT OF CONCRETE AND MASONRY STRUCTURES



MASTER THESIS

ANALYSIS OF INPUT PARAMETERS FOR NUMERICAL SIMULATIONS OF FIRE

ANALÝZA VSTUPNÍCH PARAMETRŮ PRO NUMERICKÉ SIMULACE POŽÁRŮ

BC. ŠÁRKA KOŠTÁLOVÁ

SUPERVISORS: ING. RADEK ŠTEFAN, PH.D., ING. MARTIN BENÝŠEK

2020

ZADÁNÍ DIPLOMOVÉ PRÁCE

I. OSOBNÍ A STUDIJNÍ ÚDAJE

Příjmení: Košťálová Jméno: Šárka Osobní číslo: 438975
Zadávající katedra: K133
Studijní program: Stavební inženýrství
Studijní obor: Integrální bezpečnost staveb

II. ÚDAJE K DIPLOMOVÉ PRÁCI

Název diplomové práce: Analýza vstupních parametrů pro numerické simulace požáru

Název diplomové práce anglicky: Analysis of Input Parameters for Numerical Simulations of Fire

Pokyny pro vypracování:
Rešerše literatury.
Popis modelů požáru.
Analýza vstupních parametrů.
Parametrická studie.
Modelové příklady.
Vyhodnocení.
Závěr.

Seznam doporučené literatury:

ČSN EN 1991-1-2 Eurokód 1: Zatížení konstrukcí - Část 1-2: Obecná zatížení - Zatížení konstrukcí vystavených účinkům požáru

M. Benýšek and R. Štefan. FMC - Fire Models Calculator. CTU in Prague, 2015.

A. H. Buchanan. Structural Design for Fire Safety. Wiley, 2002.

MATLAB. Version 8.6.0 (R2015b). The MathWorks, Inc., Natick, Massachusetts, United States, 2015.

K. McGrattan, S. Hostikka, R. McDermott, J. Floyd, and M. Vanella. Fire Dynamics Simulator User's Guide. NIST Special Publication 1019, Sixth Edition, 2018.

Jméno vedoucího diplomové práce: Ing. Radek Štefan, Ph.D.

Datum zadání diplomové práce: 16. 9. 2019

Termín odevzdání diplomové práce: 5. 1. 2020

Údaj uveďte v souladu s datem v časovém plánu příslušného ak. roku

Podpis vedoucího práce

Podpis vedoucího katedry

III. PŘEVZETÍ ZADÁNÍ

Beru na vědomí, že jsem povinen vypracovat diplomovou práci samostatně, bez cizí pomoci, s výjimkou poskytnutých konzultací. Seznam použité literatury, jiných pramenů a jmen konzultantů je nutné uvést v diplomové práci a při citování postupovat v souladu s metodickou příručkou ČVUT „Jak psát vysokoškolské závěrečné práce“ a metodickým pokynem ČVUT „O dodržování etických principů při přípravě vysokoškolských závěrečných prací“.

30. 9. 2019

Datum převzetí zadání

Podpis studenta(ky)

Proclamation

I, Šárka Košťálová, hereby declare that the present diploma thesis was composed by myself and that the work contained herein is my own. I also confirm that I have only used the specified resources.

Prague, Czech Republic

January 2020

.....

Šárka Košťálová

Acknowledgements

Firstly, I want to give huge thanks to my parents. Not only for *always* being there for me, but also for the immense support, both financial and psychical, throughout my whole studies. Most of the success is yours. I would never be the person I am today without you two.

Secondly, I am grateful to the family I had the luck to choose for myself, my friends. To both the Czech and the Spanish part of family, thank you for always being there for me, for giving me a hand when needed, for facing all the struggles together. Lastly, thank you for what I value the most — making sure that none of it was boring. It was a hell of a ride!

However, one of the biggest thanks belongs to my supervisors Radek Štefan and Martin Benýšek. Thank you for your time, all your help and the compassion both of you had during the studies and furthermore while developing this thesis.

Thank you.

Abstract

This thesis deals with a consideration of input parameters for numerical simulations of fire. The background section consists of the description of two essential matters – how the enclosure fire is understood by available literature and what kind of factors influence the fire development. The main mathematical models proposed by the literature, their basic concepts, and their main input parameters regarding energy input are all included in the next chapter. A sensitivity analysis of input parameters is included as following. Three mathematical models – the parametric fire curve, the zone model and the computational fluid dynamics model, described in the theoretical section, are examined to determine their assessment of an influence of ventilation to the energy and temperature progresses. A parametric curve defined in Eurocode 1991-1-2 is considered and compared to two numerical models developed by National Institute of Standards and Technology – to the zone based model CFAST and to the computational fluid dynamics model FDS. Finally, a comparison of the three models and the discussion regarding structural fire design is incorporated, as well as a concluding discussion on the topic of an appropriateness of a fire model.

Keywords

Enclosure fire; Fire Model; Fire Simulation; Ventilation; Ventilation-controlled Fire; Fuel-controlled Fire; Parametric Curve; Zone Model; Computational Fluid Dynamics.

Abstrakt

Diplomová práce se zabývá analýzou vstupních parametrů pro numerické simulace požáru. V teoretické části práce je popsáno, jak je požár v uzavřeném prostoru definován, vlivy, které požár ovlivňují, a jejich způsob působení na průběh požáru. Základní koncept hlavních matematických modelů a jejich stěžejní vstupní parametry, týkající se zadání energie, jsou zahrnuty v následující kapitole. Citlivostní analýza vstupních parametrů se nachází v další části práce. Pozornost byla zaměřena především na určení rozsahu vlivu ventilace na vývoj požáru a následně na rychlost, se kterou se energie uvolňuje a průběh teplot pro tři různé matematické modely požáru. Výsledné hodnoty byly porovnány pro model parametrické křivky, zónový model v software CFAST a CFD model FDS.

Klíčová slova

Požár v uzavřeném prostoru; Modely požáru; Simulace požáru; Ventilace; Požár řízen ventilací; Požár řízen palivem; Parametrická křivka; Zónový model; CFD.

Contents

| | | |
|-----------|--|-----------|
| 1 | Introduction | 1 |
| 1.1 | Motivation | 1 |
| 1.2 | Research Objective | 2 |
| 1.3 | Outline | 2 |
| I | Theoretical Basis | 3 |
| 2 | Fire and Influencing Factors | 4 |
| 2.1 | Pyrolysis Process and Gas Phase Combustion | 4 |
| 2.2 | Fire Development | 4 |
| 2.3 | Factors Influencing Fire | 6 |
| 2.3.1 | Energy | 6 |
| 2.3.2 | Ventilation | 11 |
| 2.3.3 | Geometry | 13 |
| 2.3.4 | Surrounding constructions | 13 |
| 2.3.5 | Ignition Source | 14 |
| 3 | Mathematical Models of Fire | 15 |
| 3.1 | Parametric Fire Curve | 16 |
| 3.2 | Zone Model | 18 |
| 3.3 | CFD Model | 21 |
| 3.3.1 | Energy Input | 22 |
| 3.3.2 | Outputs | 26 |
| II | Analysis of Input Parameters for Numerical Fire Simulations | 27 |
| 4 | Analysis of Input Parameters | 28 |
| 4.1 | Compartment | 28 |
| 4.2 | Energy Input | 30 |

| | | |
|----------|---|-----------|
| 4.3 | Parametric Curve Analysis | 30 |
| 4.4 | Zone Model CFAST | 32 |
| 4.4.1 | Energy Input | 33 |
| 4.4.2 | Energy Outputs | 35 |
| 4.4.3 | Temperature Outputs | 38 |
| 4.5 | Fire Dynamics Simulator | 44 |
| 4.5.1 | Compartment Geometry and Mesh | 45 |
| 4.5.2 | Ventilation | 45 |
| 4.5.3 | Energy Input | 46 |
| 4.5.4 | Energy Outcome | 48 |
| 4.5.5 | Temperature Outcome | 57 |
| 4.6 | Discussion about Fire Models with Respect to Structural Fire Design | 61 |
| 5 | Discussion | 65 |
| 6 | Conclusion | 67 |

Nomenclature

| | |
|-----------------------|---|
| ΔH | heat of combustion |
| ΔH_{02} | heat of combustion based on oxygen consumption |
| $\Delta h_{f,\alpha}$ | heat of formation of the lumped species α |
| \dot{m}_e | entrainment rate inside the fire plume |
| \dot{Q} | heat release rate |
| \dot{m}'''_{α} | mass production rate of the lumped species α |
| \dot{q}''' | heat release rate per unit volume |
| \dot{q}_i | is rate of addition of heat into layer i |
| λ | thermal conductivity of a material |
| \bar{p}_m | background pressure |
| ρ_{ijk} | desity of cell ijk |
| τ | equivalent duration of fire, defined in CSN 73 0804 |
| c | heat capacity of a material |
| C_{LOL} | smoothing function ranging from 0 to 1 [-], depending on the fraction of oxygen in the layer containing fire and on limiting oxygen mass fraction |
| c_p | heat capacity of air at constant pressure |
| h_0 | height below neutral axis while analysing pressure differences outside and inside of burning compartment |
| h_F | height under neutral axis while analysing pressure differences outside and inside of burning compartment |
| R | universal gas constant |
| V_i | total volume of i -layer in a investigated compartment |
| W_{α} | molecular weight of gas species α |

Y_{O_2} mass fraction of oxygen in the layer containing the fire

$Z_{\alpha,ijk}$ species mixture α of cell ijk

m_i total mass in gas layer i

T gas temperature

The nomenclature is consisted of terms utilized by different fire models used for analysis in this thesis.

1. Introduction

The trend of the demand regarding sizes and heights of structures is growing. The established approaches to fire safety design, such as national standards fire safety evaluation, are often inadequate. Due to this fact a performance-based fire design comes to the forefront of fire safety engineering and structural fire design.

The performance-based fire design is a rapidly developing discipline which aims to understand and describe the fundamental physical phenomena occurring during the fire situation. Generally, the field of study idealizes the development of a potential real fire that could emerge in a given space, or a fire that happened in the past. It deals with a detailed evaluation of an emergence and subsequent development of fire and the rate of creation, spread of smoke, and combustion products. Then a discrete data, such as temperature and heat flux, which need to be implemented as input data into subsequent mechanical analysis model are obtained.

An array of fire models varying in number and details of input data, type of mathematical apparatus used, and the accuracy of output data, is available. Independently of the fire model choice, it is essential to determine the factors that affect the fire and to determine how the initiation and development of fire is affected. From experiences with devastating fires throughout the history and acquired scientific knowledge from the past decades, it is known that fire is influenced by a number of factors. More specifically, regarding the variations of the compartment geometry, the ventilation conditions in the enclosure and consequent amount of available oxygen, type, quantity and distribution of present fuel, type and thermally-dependent characteristics of the surroundings constructions, it also depends on the size and position of the ignition source. All these factors are currently the subject of scientific research to accurately assess the outcomes from a potential fire in an investigated enclosure.

1.1 Motivation

As the trends of fire safety design is slowly moving toward fire modelling rather than standardised approach, it is obligatory to be constantly keeping up with the progress. It is completely essential to understand fundamental mathematical, physical and chemical processes directing the fire model to be able to assess the influence which could cause a little variation within the input data to the outcome of the analysis. Consequently, a more accurate determination of an input data for following mechanical response analysis of a structure can be gained. Thus, a more effective solution regarding structural design can be implemented.

1.2 Research Objective

This thesis aims to emphasize the differences between three fire models - parametric curve, zone model, and computational fluid dynamics model - in terms of ventilation influence to energy progress assumption. Then, a more detailed examination of computational fluid dynamics model was conducted to assess the variations within outcomes from simulations with different combustion gases assumptions, also in relation to ventilation.

1.3 Outline

The work consists of two main parts. The first part explains the theoretical background including fire phases and factors influencing fire development. It has a detailed look into energy and ventilation, and emphasizes the difference between the pyrolysis process and the combustion process. A brief summary of existing fire models with emphasis to models used in the coming part follows. The second - empirical part examines an extent of an influence of a size of an opening area to energy and temperature progresses in three different mathematical fire models. The parametric fire curve from Eurocode 1991-1-2 is compared to the zone model based software CFAST and the computational fluid dynamics based software Fire Dynamics Simulation.

Part I

Theoretical Basis

2. Fire and Influencing Factors

To ignite a material, three fundamental conditions needs to be fulfilled. *First*, a sufficient amount of combustible gases have to be injected into the compartment from the preheated solid or liquid. *Second*, these combustible gases needs to be mixed with the oxidant (oxygen). *Third* the mixture have to be provided with a source of a spark (electric spark, heated wire ..) to locally heat a minimum quantity of the mixture or needs to have a high temperature itself to induce autoignition. [6]

2.1 Pyrolysis Process and Gas Phase Combustion

The generation of thermal energy causes a raise in the temperature of the solids. As the temperature continues to elevate a disruption of a structure occurs (chemical bonds breakage, the material degradation) and releasing of volatile gases into the ambient atmosphere starts. This process is referred to as *pyrolysis process*. Subsequently the burning itself occurs at the moment when the volatile gases mix with the oxidative atmosphere (the air in most cases) and the mixture is heated to a ignition temperature. This process is referred to as *gas phase combustion*. A graphic outline of the two processes is contained below. [21]

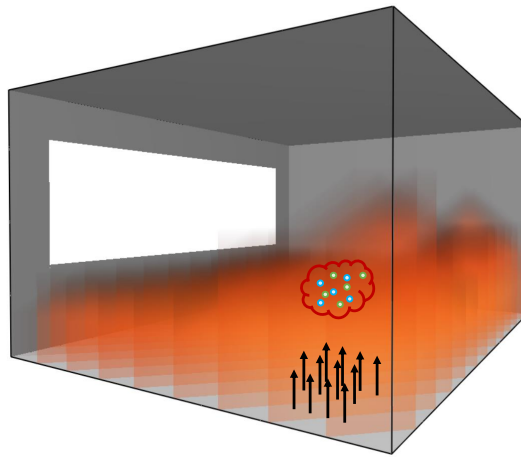


Figure 1: A graphic illustration of a difference between the process of pyrolysis and gas phase combustion.

2.2 Fire Development

After the ignition the fire grows and can develop in a number of different ways. The way of development mostly depends on the enclosure geometry, ventilation and thus the amount of available oxygen,

type, amount, and surface area of the fuel and the type and material properties of the boundary constructions. [14]

In principle one of three things may happen. If the fire is local, it may burn itself out without spreading to other combustible material (particularly if the item first ignited is in an isolated position), if there is inadequate ventilation, the fire may self-extinguish or continue to burn at a very slow rate, or if there is sufficient fuel and ventilation, the fire may progress to full room involvement in which all exposed combustible surfaces are burning. [7]

The last mentioned can be divided in terms of enclosure temperatures into 5 fundamental stages [14]:

1. *Ignition* is the moment of a start of exothermic reaction generating the thermal energy and producing combustion products,
2. *Growth*, when the fire may grow at a slow or fast rate, depending on the type of combustion, the type of fuel, influence by the surrounding constructions and oxygen availability,
3. *Flashover* is the rapid transition to a state of total surface involvement in a fire of combustible material within an enclosure, as defined by the International Standards Organization [24],
4. *Fully developed fire*, which is defined by the biggest energy release and it is often limited by the availability of oxygen and thus referred to as ventilation-controlled fire,
5. *Decay*, is the last phase of enclosure fire when the fuel is being consumed, the released energy decays and average gas temperature declines. The burning regime may change from ventilation-controlled back to fuel-controlled.

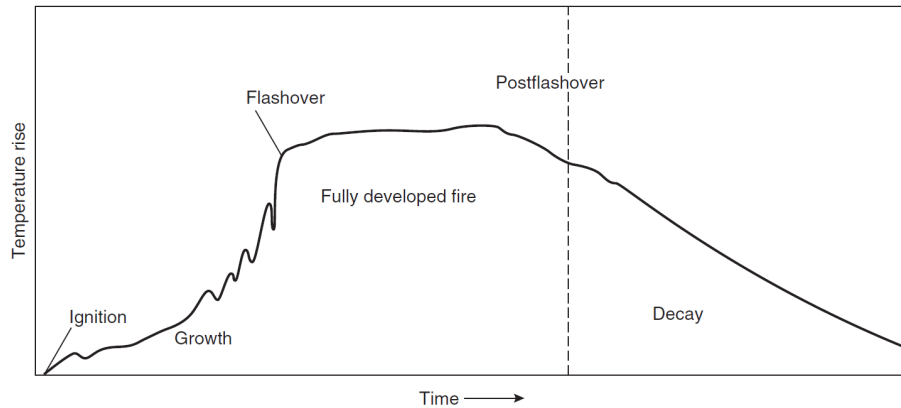


Figure 2: Fire development stages with regards to temperature progress within the compartment. Reprinted from [6].

Flashover is not a precise term and several experimental studies were carried on to assess the onset of flashover. Three basic criteria are stated for flashover to appear. The criteria given usually demand

that the room temperature near the ceiling has reached 500–600 °C, the heat flux is about 20 kW m⁻² at floor level or that flames appear from the enclosure openings. The part of fire development before flashover is referred to as pre-flashover stage, the fully developed fire and its decay phase are being referred to as post-flashover stage of fire. [7]

2.3 Factors Influencing Fire

Factors influencing the fire initiation and its development may be divided into two main categories. The first includes factors dependent on the enclosure itself – geometry, material of surrounding constructions and its characteristics and shape and location of openings. The second category consists of factors depending directly on fuel – type, amount, spacing and orientation of combustible material and size and location of the ignition source. [14]

2.3.1 Energy

Because of the need to distinguish technical terms, rather than discussing fuel definition author is using energy as an specific term by which is referring to the possible energy release by the present combustibles in potential fire situation.

Without any doubts defining the energy potential is one of the most challenging tasks within fire simulation which need to be paid attention to. Depending on the fuel type, its placing and of course the amount, the energy potential will vary. The energy potential of present fuel is represented by heat release rate (sometimes referred to as a rate of heat release). Heat release rate expresses the amount of overall thermal energy released and rate at which the combustion reactions produce the energy. There are few approaches to insert this information to mathematical fire software. These approaches are chosen on the basis of users knowledge about the present fuel, desired accuracy of outputs and modelling and calculation time demands.

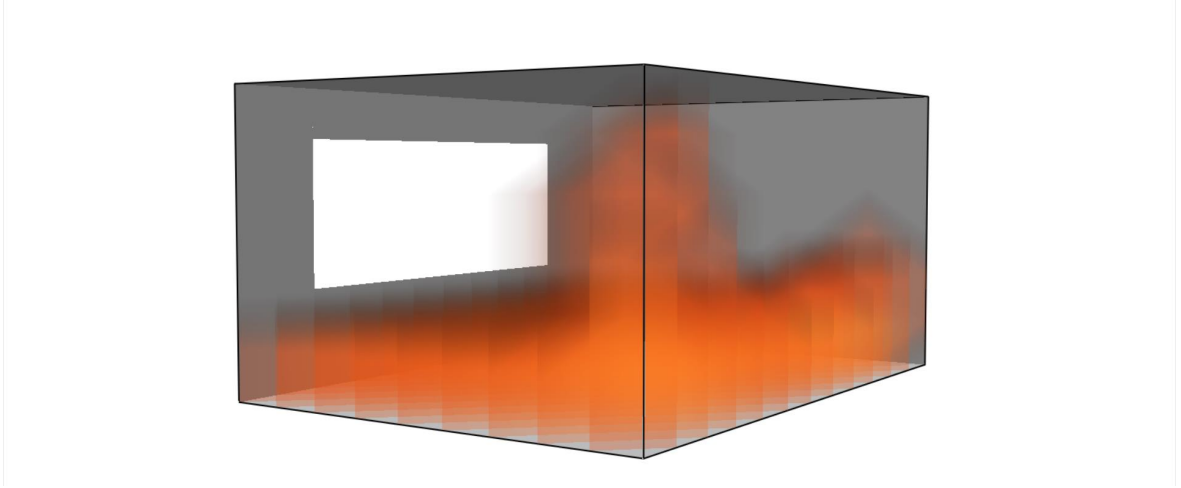


Figure 3: An energy input defined by pyrolysis prescription over the compartment's floor.

The first approach to fire determination is using the standardized values expressing the fire potential. For the Czech Republic as a European union member a standardized values of fire energy potential from Eurocode 1991-1-2 [8] or codes CSN 7308xx¹ can be used as a reference to fire potential assumption.

As for Czech standards a values of kg m^{-2} of reference wood is specified for different occupancies or the time of fire duration τ_e also referencing to kg m^{-2} according to its occupancy. Thus a wood cribs can be modelled in the examined compartment, and the fire spread determined by the performance-based procedure.

Regarding European codes, for compartment fires values of fire load densities are stated in table E.4 depending on the occupancy of the compartment, or in case of occupancy missing can be assessed individually following steps described in part 2.6. The determination is based on a survey performance of loads, local arrangement and its variation in time most preferably compared to already existing project with particularly specified differences based on the requirement and other demands by the client between them. [8] For the numerical simulation however clearer specification of the heat release progress is needed, specifically the rate, on which the energy is being evolved. For that a simplified analytic definition called t-squared fire can be used.

T-squared fire curve determines the rate of heat release and consists of 3 parts, growing phase, horizontal plateau and decay phase.

Growing phase, sometimes referred to as pre-flashover phase is defined by expression

$$\dot{Q}(t) = 10^6 \cdot \left(\frac{t}{t_\alpha}\right)^2, \quad (2.1)$$

where

¹The last two digits determine the code area of interest. They are provided by CAS for a fee and are available on [23].

- $\dot{Q}(t)$ is heat release rate [kW],
- t is time of fire development [s],
- t_α is time [s], at which the fire reaches 1 MW. In [8] four values are given for *slow*, *medium*, *fast* and *ultra-fast* fires. These values are included in Table E.5 and are defined for a limited number of occupancies.

The first phase growth is limited by the second phase, which is a constant layer referred to as a horizontal plateau. Horizontal plateau or maximum heat release rate Q , is being obtained from equation $RHR_f \cdot A_{fi}$. The values of RHR_f are given in Table E.1 [8]. However, the equation is only valid when the fire has enough oxygen to consume and is thus fuel-controlled (see 2.3.2).

The third, decay phase, starts its linear decrease when 70% of the total fuel has been consumed and reaches the zero level of energy release when the whole fire load has been completely burnt. Mathematically speaking, the decay starts after 70% of total energy has been already released. The total energy is expressed by the area indicated by curve. Thus, when the sum of areas indicated by the growing phase and horizontal plateau reaches the 70%, the energy release rate starts its decay.

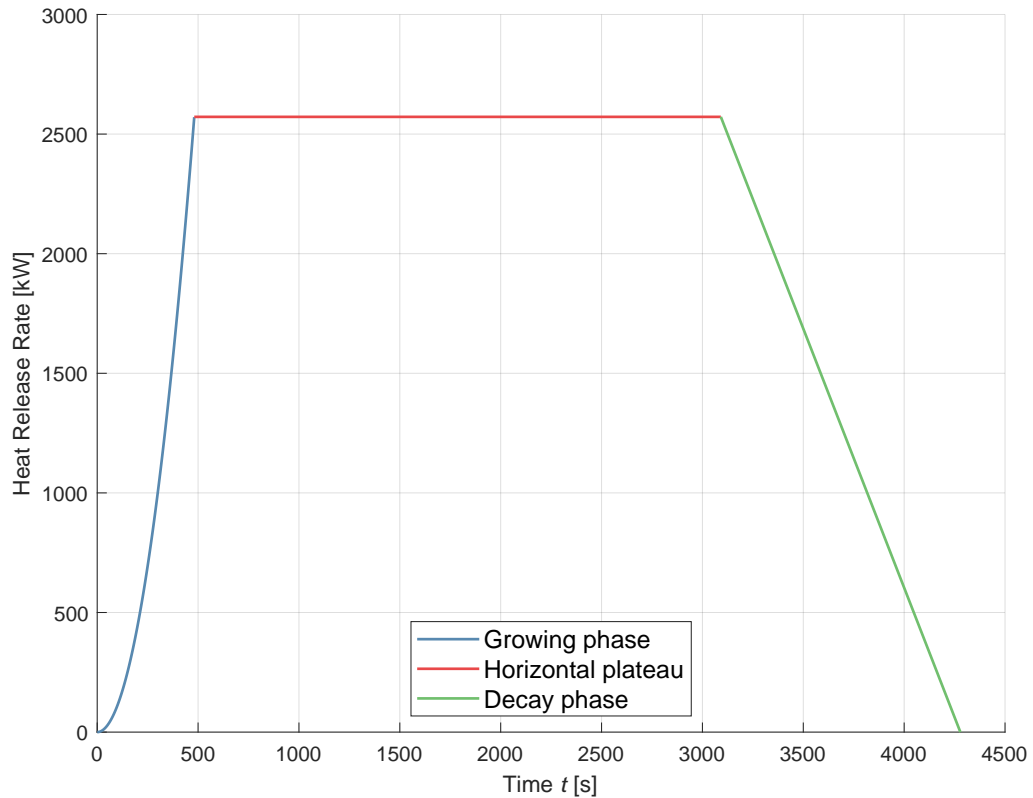


Figure 4: An example of t -squared fire curve for a hotel room.

However, in any case it is essential to assess whether there is enough oxygen available in the compart-

ment. If the fire lack the oxygen, the plateau level has to be reduced following the available oxygen content. There are two options to reduce the maximum energy released. It is possible to assess the value automatically in zone model based software or by simplified expression: [8]

$$\dot{Q}_{max} = 0.1 \cdot m \cdot H_u \cdot A_v \cdot \sqrt{h_{eq}}, \quad (2.2)$$

where

- \dot{Q}_{max} is maximum level of the rate of heat release [kW],
- m is the combustion factor representing the combustion efficiency [-] $m = 1$ for highly flammable materials, $m = 0$ for non-combustible materials. For cellulosic materials a value of $m = 0.8$ is assumed,
- H_u is the net calorific value of wood with $H_u = 17.5 [MJ/kg]$,
- A_v is the opening area [m^2],
- h_{eq} is the mean height of the openings [m].

If inequality $\dot{Q}_{max} < Q$ stands, the maximum heat release rate is restricted, we are referring to the fire as to ventilation-controlled. It is necessary to bear in mind that if the fire curve maximum (horizontal plateau) is restricted then the decay phase must be extended accordingly so the energy released during the fire is maintained².

In Figure 5 a comparison of a progress of fuel-controlled and ventilation-controlled curves is included. The only changed input is the opening area and consequently the availability of oxygen in the compartment. The reduction of the horizontal plateau is determined by Equation 2.2.

²Energy released during the fire [kJ] is the area below the curve.

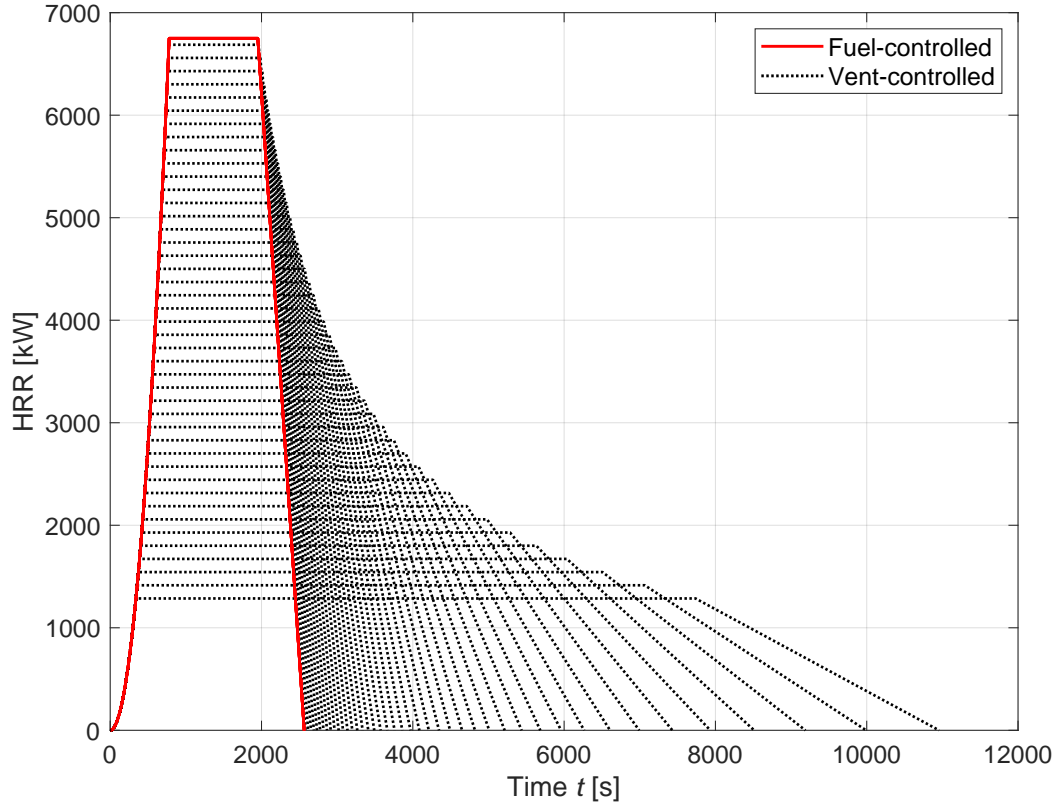


Figure 5: Illustration of t -squared fire progresses. Red colour illustrates fuel-controlled fire (with enough amount of oxygen), while the black color stands for ventilation-controlled curves whose horizontal plateau have been restricted by Equation 2.2.

The second approach to energy definition is a precise definition of combustible material present in the enclosure. For this definition usually more specific and extensive knowledge about the material characteristics, ignition temperature and fire spread are required, depending on the type of fire model and software, in which the analysis is being conducted. However, to emphasize the importance of following, it always closely depends on accessibility of input data and on an extent with which the available data have been simplified. Requirements on the output type and its attention to detail also need to be determined and are closely connected to the above mentioned inputs definition.

HRR of an combustible object or a material can be calculated from Equation 2.3 or by direct measurement in open-burning HRR calorimeters or room fire tests. [6]

$$\dot{Q} = \dot{m}_f \cdot \Delta h_c, \quad (2.3)$$

where

· $\dot{Q}(t)$ is heat release rate [kW],

- \dot{m}_f is burning rate [kg/s],
- Δh_c is effective heat of combustion³ [kJ/kg].

There are two general ways how to obtain effective heat of combustion. It can either be determined by theoretical relation or by physical experiments. However, in practice the effective heat of combustion is not a constant, so experimental techniques normally involve directly measuring the HRR, rather than using Equation 2.3. [6]

Fire growth data for solid burning items is available from several sources, such as National Fire Protection Association Handbooks [1], Standard Reference Database of National Institute of Standards and Technology [5] or Material Property Data [19]. Besides other characteristics they include energy release rates for many different types of materials, also incorporates species production rates, which can be used for calculation of species concentrations in examined compartment.

2.3.2 Ventilation

The amount of energy released in a compartment is closely dependent on the rate of supply of oxygen. Knowledge of the ventilation conditions can therefore be used to evaluate the maximum rate of energy release inside a compartment. If the oxygen availability is not adequate, the fire quickly becomes oxygen-starved and may either self-extinguish or continue to burn at a very slow burn rate which pace then depends on the availability of oxygen. The crucial elements for the fire development are the size, shape and position of openings in the enclosure.

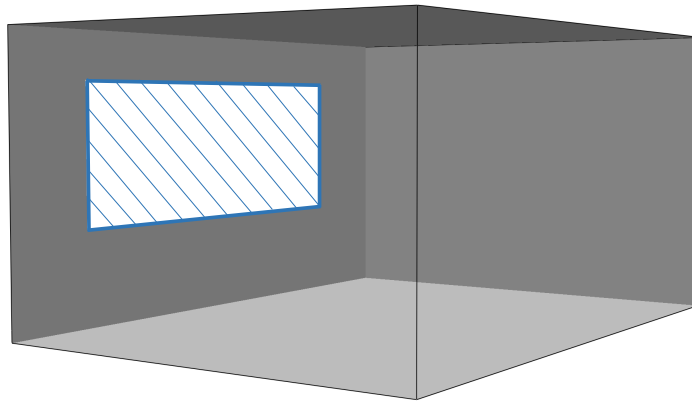


Figure 6: Illustrative caption of emphasizing the influence of the size of the compartment's opening.

The way of influencing the fire depends mainly on the fire phase. In the growing phase when the fire is fuel-controlled its development depends closely on the ability and efficiency of the openings to remove the hot gasses out from the enclosure. When the hot gasses are removed, the thermal feedback

³Energy content of the combustible material.

to both constructions and other combustibles diminishes. The efficiency of hot gases exhaust is being determined by position and height of the opening. However when fire becomes controlled by the availability of oxygen the opening size and shape become all-important. It has been shown both by experimental research and theoretical analysis that the rate of burning of ventilation-controlled fire depends strongly on ventilation factor defined as $A_W \cdot H^{1/2}$ where A_W is an opening area and H is its height. [14]

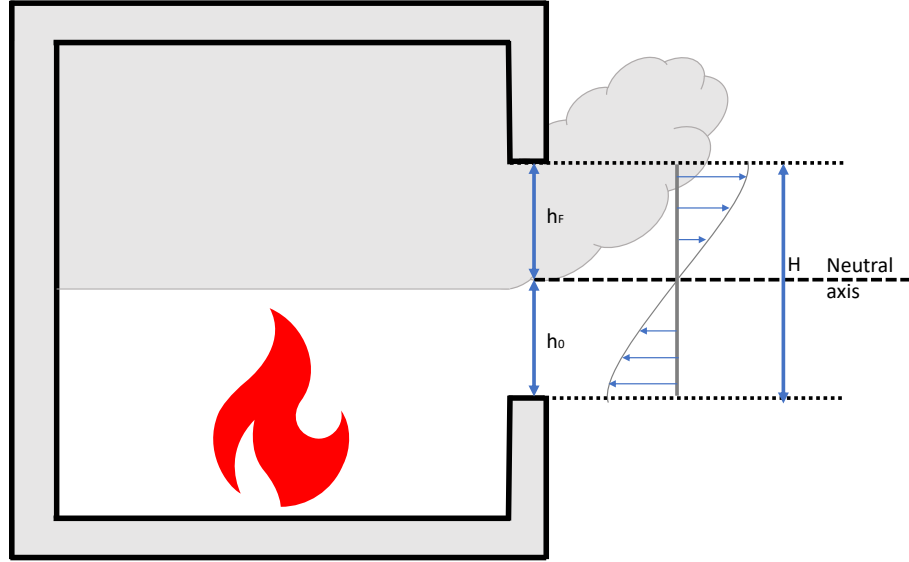


Figure 7: Distribution of flow income and discharge assumed by theoretical analysis of pressure difference when deriving the ventilation factor. h_F refers to the part of window, where only a discharge of the hot gases takes place. h_0 indicates the part, where the cold air enters the room. According to [14].

Ventilation factor defined as $A_W \cdot H^{1/2}$ was introduced in the first systematic study of fully developed compartment fires, when mass loss rate was found to depend strongly on the size and height of the ventilation opening. If the factor is increased, the heat release rate is increased. This applies up to a certain limit when the heat release rate becomes independent of the ventilation factor. Thus, two separate burning regimes were defined. If the correlation between ventilation factor and heat release rate stands, we call the fire ventilation-controlled. After the rate of energy evolved becomes independent of the ventilation factor, we are referring to the fire as fuel-controlled. The same relation is derived from analysis of a pressure difference of the compartment and outside of the burning space. The driving force of the gas flow is buoyancy caused by gas pressure difference of gases inside the burning space and outside, which is a direct consequence of the high temperatures in the compartment. More of this topic with a derivation of the relation is included in [14].

So to distinguish between fires directed by different burning regimes, as stated in SFPE Handbook of Fire Protection Engineering [6], **fuel-controlled fire** is such a fire, where a sufficient amount of oxygen is available to react with all the fuel within the enclosure. On the contrary **ventilation-**

controlled fire is defined as the fire, where the energy release rate is limited by the amount of available oxygen. Some of the pyrolysis products (unburned fuel) leave the compartment and can react outside where oxygen is available.

2.3.3 Geometry

The geometry variations of enclosure can have smaller or bigger influence to the development of fire. When comparing the overall sizes of compartment, the same fuel (amount, location, ..) burning in a small compartment with low ceiling will cause rapid fire growth and rather high temperatures. The hot smoke layer is produced quicker and thus can heat up the ceiling and parts of surrounding surfaces, which will radiate toward the burning items. Additionally, the fire plume could reach the ceiling and spread horizontally, heating the construction directly.

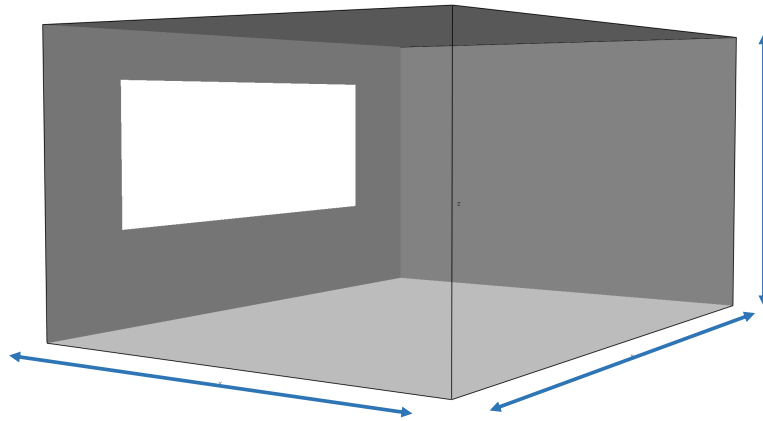


Figure 8: Illustrative caption of emphasizing the influence of the geometry of compartment.

For bigger compartments the smoke layer development will generally be slower, lower gas temperatures and thus the slower rate of heat release. However even in more extensive spaces, the hot layer of smoke and under the ceiling can heat up the combustible items present in the compartment and result in rapid fire spread. [14]

2.3.4 Surrounding constructions

As follow-up of the previous part, the material and thickness of surrounding construction can influence the fire development considerably. Speaking about non-combustible construction materials (such as concrete) a term thermal inertia is defined. It is formed by multiplying material's conductivity k , density ρ and heat capacity c .

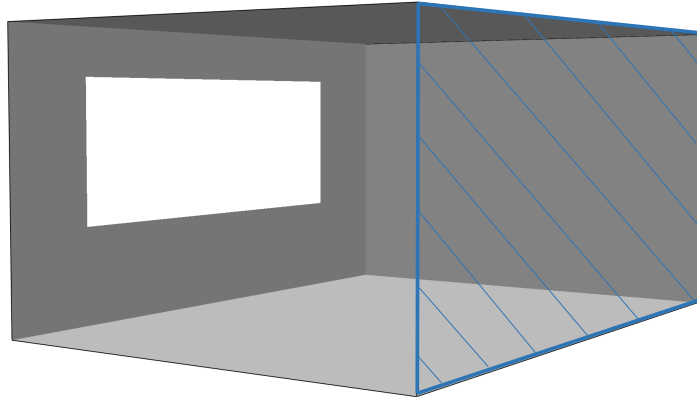


Figure 9: Illustrative caption of emphasizing the influence of the type, characteristics and width of the compartment's surrounding constructions.

Material with low thermal inertia keep out the heat energy and consequently majority of the energy remains accumulated within the layer of the hot gases. Conversely, for materials with high thermal inertia allow the heat energy to be stored within the material and is thus reducing the thermal energy and temperatures within the hot gas layer.[14]

2.3.5 Ignition Source

The size, location and type of the ignition source influence the development of enclosure fire. The growth and following progress Generally, the bigger the ignition is, the faster the growth of the initial fire is. [14]

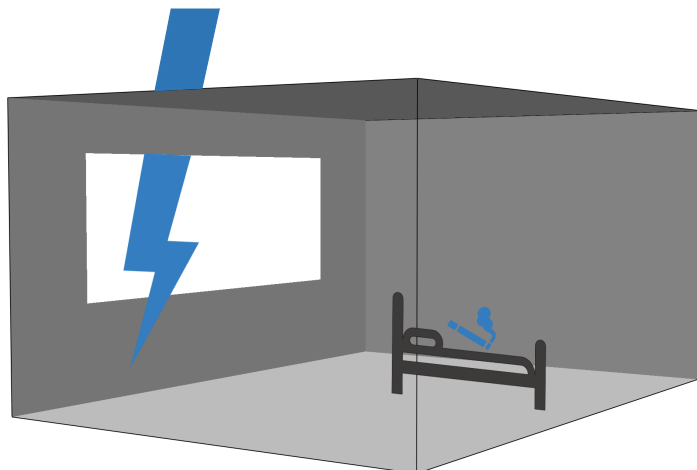


Figure 10: Illustrative caption of emphasizing the influence of the size, type and location of the ignition source.

3. Mathematical Models of Fire

There are two options to describe a fire and its outcomes. The first one is to set a *physical model*, either real scale or simplified. The latter one is being preferred mostly due to usually much higher costs of the real scale models. Findings discovered on basis of physical models form solid fundamentals for upcoming theoretical research and definition of mathematical relations. The second option is *mathematical model* approach, which, in principle, is an engineering approximation of time-varying conditions originated from fire. [12]

By mathematical modelling it is possible to quantify and define the parameters needed for the fire safety design, including structural fire design. Fire safety design analysis is being defined by time-dependent variables, such as heat release rate, temperature of hot gases in enclosure, time to flashover, smoke intensity and size of the fire, depending closely to a type of assessment conducted. The analysis of fire development can be classified either into stochastic or probabilistic class type of fire model. *Stochastic models* are often referred to as probabilistic models. This type is treating the fire development as a series of steps. Each step is being assigned a probability, which is determined on basis of a physical models, an analysis of a historical fire situation, or based on previous analytical research. This probability governs the transition from one event to another (for example transition from ignition to established burning). Conversely, *deterministic models* describe the fire phenomena by mathematical expressions based on physics and chemistry. Although many simplifications and assumptions are being made, many mathematical models are providing precise enough estimation of the fire effects. [6]

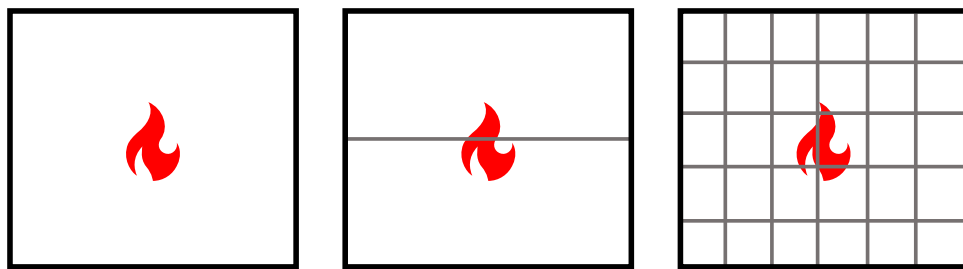


Figure 11: Spoiler illustration of a difference between fire models discussed below. It exemplify parametric fire curve model, zone model and field type model.

3.1 Parametric Fire Curve

Parametric fire curve is basic analytic temperature-time history model. In principle it is a very simple one control volume model assuming the whole compartment to be well-stirred reactor. Thus a number of limitation of the examined compartment must be made in order to maintain sufficient accuracy of the results. These limitation will vary depending on the type of parametric curve used. The brief history of the parametric fire curves development and the main parametric curves (as there is not only one) are included in Kucera's diploma thesis [16].

The fundamental concept of parametric fire curve is solution of an equation of heat balance conservation: [7]

$$\dot{q}_C = \dot{q}_L + \dot{q}_W + \dot{q}_R + \dot{q}_B, \quad (3.1)$$

where

- \dot{q}_C is rate of heat release due to combustion,
- \dot{q}_L is rate of heat loss due to replacement of hot gases by cold,
- \dot{q}_W rate of heat loss through the walls, ceiling and floor,
- \dot{q}_R rate of heat loss by radiation through the openings,
- \dot{q}_B rate of heat storage in the gas volume (neglected).

Within the structural fire design the main interest is focused to the stage of fire, when the structural damage can occur. For parametric fire curve the pre-flashover stage may be neglected as average temperatures are relatively low. So in subsequent calculations, the time 0 refers to the start of the fully developed fire.

The elements taking part in the heat balance equation stated above are illustrated in Figure 12.

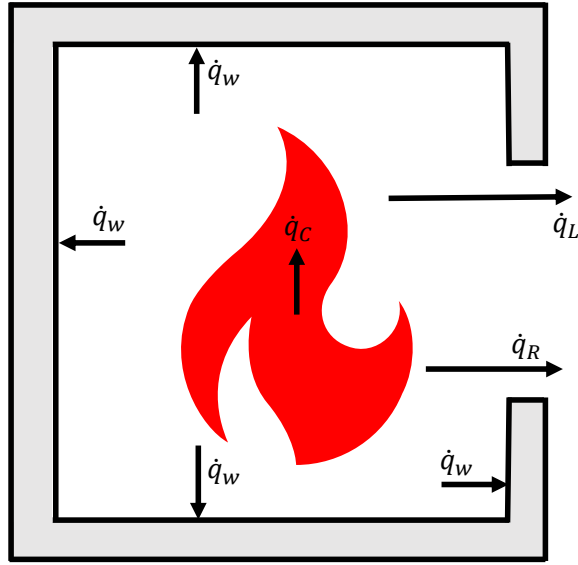


Figure 12: Heat losses and gains during a fully developed compartment fire. The source of energy is \dot{q}_c , which is rate of heat release due to combustion. The energy losses are \dot{q}_L , which is rate of heat loss due to replacement of hot gases by cold, \dot{q}_w rate of heat loss through the walls, ceiling and floor and \dot{q}_R rate of heat loss by radiation through the openings. According to [7].

For the analysis in Part II of this project, the parametric fire curve defined in Eurocode 1991-1-2 [8] is being considered. As the work is mostly focused to numerical fire models rather than analytic description of fire, the process of the curve's progress determination is not included. The parametric curve is used to demonstrate burning regime assessment with comparison to different fire model. The curve definition is described in detail and calculated step by step in Kucera's thesis [16], also showing variation in the curve progress while deviating the inputs of the curve prescription. Restriction values for each input is discussed as well. Restriction regarding the investigated compartment are following. The maximum area of the examined compartment can not overreach 500 m². There must not be openings in the overhead construction, meaning ceiling or a roof and the maximum height of the ceiling must not be larger than 4 m.

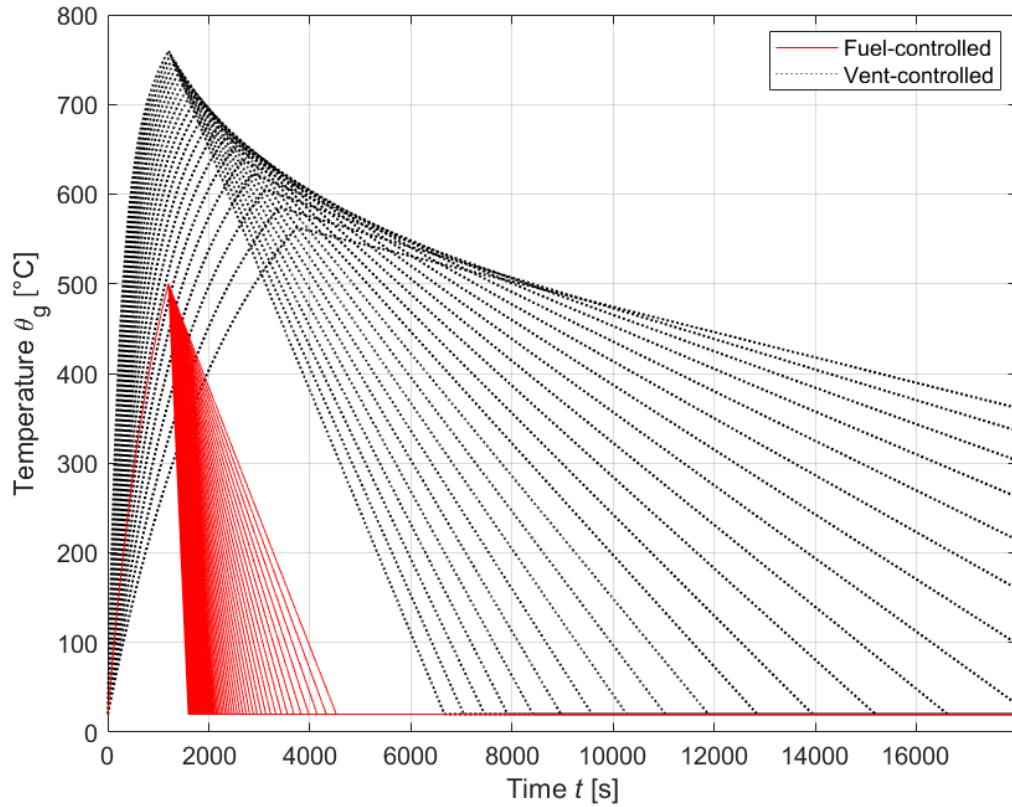


Figure 13: Illustration of parametric curve progresses for the ventilation factor $O = \langle 0.02; 0.2 \rangle$ with a 0.002 step.

In principle, parametric fire curve is defined by two key prescriptions, depending on burning regime. In Figure 14 parametric curves both fuel and ventilation-controlled are contained to illustrate the difference within the progresses. The progresses applies for a compartment with only one input parameter deviating - the area of the compartment openings. The rest of parameters remain constant.

3.2 Zone Model

Zone models or control volume models divide the compartment into one control volume when the fire is in its post-flashover stage. Thus the whole compartment is thought of as well-stirred batch reactor. Two control volumes are considered for pre-flashover stage of fire, upper, hot layer and lower, cooler layer. The way in which heat and mass are exchanged between two control volumes is the fire plume. The majority¹ of the energy released by fire is transported by convection into the upper layer by the plume. The plume rises and entrains cooler air from the lower layer. That reduces its temperature and increases the mass flow rate. In principle, for these physically justifiable control volumes conservation

¹65% - 75% depending on the literature used and the fire model considered.

equations are being solved, while the conservation of mass and oxygen provide additional support equations. [20]

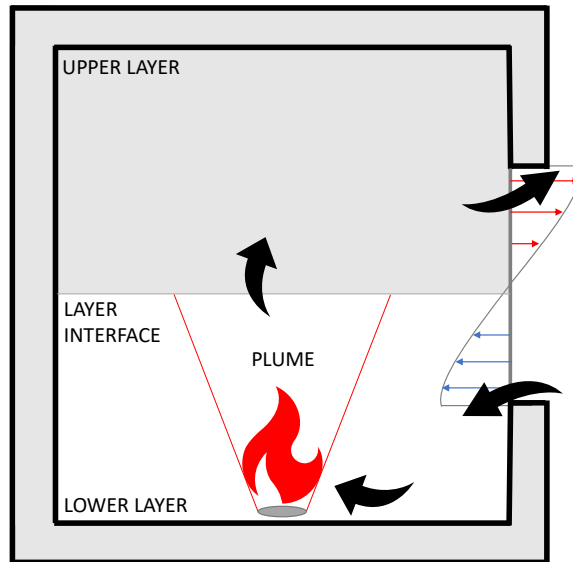


Figure 14: Basic principle of zone model. According to [4].

A number of zone model based software exist, varying more or less in the fire phenomena assumption. An overview of representative zone fire models is included in section 3 chapter 7 of SFPE Handbook. [6]

Neither of the available zone model based software is applicable to every type of a fire situation. The key issue regarding the determination of the most suitable software for specific analysis is the model validation data. More specifically the comparison between the model validation data with the experimental data from physical models, and thus understanding the simplification and limitation of the particular model. The evaluation of a model assumption is essential for the outcomes' accuracy. [6]

One of the zone-based models is a software CFAST or Consolidated Fire and Smoke Transport. The software is able to predict the time-evolving characteristic during user-prescribed fire, such as temperature or distribution of smoke within a compartment. It is possible to build a multi-compartment structure as the calculation of the mass transport between the compartments are implemented in the mathematical apparatus of the software as well. [4]

The software is being developed by National Institute of Standards and Technology of the United States Department of Commerce, it is free and open-source. It abounds with a wide user support and discussion forum with the developers themselves contributing as well. The download links, documentation of background calculations, discussion forum links and more are included at the website of NIST [25].

The basic concept is the horizontal distribution of the compartment into upper and lower layer. The fire directs the movement of combustion products from the lower to the upper layer via fire plume. [4]

Fire plume is a buoyant flow of hot gases in the flame surrounded by cold gases. The hotter and less dense mass rises upward due to density difference. [14]

The temperature within both upper and lower layer is uniform, and the evolution in time is described by a set of ordinary differential equations derived from the fundamental laws of mass and energy conservation. [4]

Within consolidated Fire and Smoke Transport (CFAST) the heat release rate is being calculated from equation

$$\dot{Q} = \min (\dot{m}_f \cdot \Delta H_c ; \dot{m}_e \cdot Y_{O_2} \cdot C_{LOL} \cdot \Delta H_{O_2}), \quad (3.2)$$

where

- \dot{Q} is heat release rate [KW],
- ΔH is heat of combustion [kJ/kg],
- \dot{m}_e is entrainment rate inside the fire plume [kg/s],
- C_{LOL} is the smoothing function ranging from 0 to 1 [-], depending on the fraction of oxygen in the layer containing fire and on limiting oxygen mass fraction taken as 0.15 by default,
- Y_{O_2} is the mass fraction of oxygen in the layer containing the fire [-],
- ΔH_{O_2} is the heat of combustion based on oxygen consumption. The representative value for typical hydro-carbon fuels is assumed to be 13,1 [MJ/kg].

The first component of Equation 3.2 refers to fuel-controlled fire, when the amount oxygen available is sufficient. The pyrolysis rate rate of fuel \dot{m}_f is being calculate from a simple equation $\dot{m}_f = \frac{\dot{Q}}{\Delta H}$, where \dot{Q} is the user-specified heat release rate.

The second component of Equation 3.2 stands for rate of heat release within the ventilation-controlled fire. It is assumed that the pyrolysis rate does not change, however not all the pyrolyzed fuel burns. Any unburned fuel is being tracked by the model as it is being transported by fire plume to upper layer or from one compartment to another. It may burn later in the upper layer or at vents if the fulfill the condition of sufficient temperature and availability of oxygen. [4]

Temperature of both the upper and the lower layer is solved by differential equation: [4]

$$\frac{dT_i}{dt} = \frac{1}{c_p m_i} \cdot (\dot{q}_i - c_p \dot{m}_i T_i + V_i \frac{dP}{dt}), \quad (3.3)$$

where the terms with lower index i apply for both lower and upper layer characteristics. Those are

- T_i is gas temperature of i -layer [$^{\circ}\text{C}$],
- c_p is the heat capacity of air at constant pressure $\text{J kg}^{-1}\text{K}^{-1}$],
- m_i is total mass in gas layer i [kg],
- \dot{q}_i is rate of addition of heat into layer i [kW],
- V_i is total volume of i -layer in a compartment [m^3],
- P is pressure at floor level of a compartment [Pa].

3.3 CFD Model

The most recent mathematical model is basically a system of coupled partial differential equations. It works on a principle of dividing continuum into definite number of control elements, calculating equations of mass, momentum and energy for each element. This model evolved outside the fire discipline and has been imported into it later a contrary to zone models which were developed inside the fire community. It should also be stressed that field models require substantial hardware resources and are often more complex to use. [6]

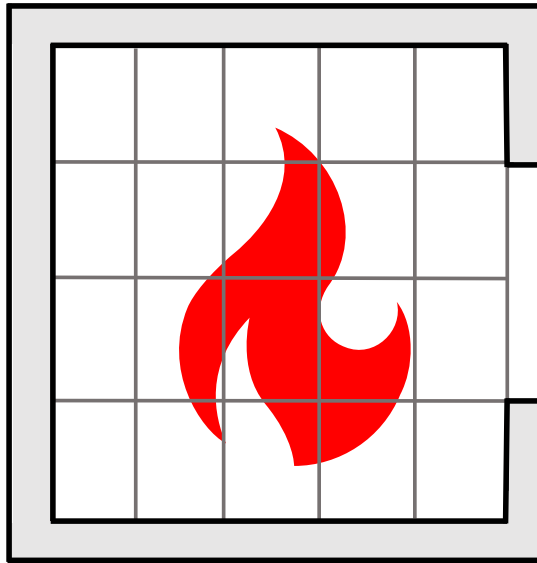


Figure 15: Illustration of a mesh in CFD model.

One of computational fluid dynamics based model is Fire Dynamics Simulator developed by by the National Institute of Standards and Technology (NIST) in cooperation with VTT Technical Research Centre of Finland. Similarly to NIST-developed zone model CFAST, FDS is in the public domain – it is free and open-source. It was first released to public in 2000 and since then numerous improvements

have been implemented, based largely on feedback of its users. An online discussion is also available to its user's. It is a tool providing solution of practical fire problems regarding fire protection engineering and the possibility to study fundamental fire dynamics and combustion.

A user-defined text file is employed as an input file from which all the parameters necessary for numerical solution of the governing equations are read. The user-specified output data are written to files. FDS itself doesn't have the user interface however is accompanied by Smokeview which is able to read FDS's output files and produce animations of the results. There are also third-party programs with user interfaces able to generate text file including the input parameters. [27]

3.3.1 Energy Input

When defining an energy input, FDS distinguishes between the process of pyrolysis and combustion of gaseous products and it is commonly causing a confusion among the users. Basic concepts of both processes are stated in section 2.1, the definition within FDS of both processes are discussed below.

FDS uses two main approaches of describing the pyrolysis process. **Both of them consider injection of calculated quantities of gaseous fuel into the compartment.** Choosing the right pyrolysis model depends on the availability of the material properties, consideration of different conditions influencing the pyrolysis process and the appropriateness of the model itself. [21]

The most simple way of pyrolysis model definition is specifying a gas burner of a given heat release rate. By this approach fire is modeled as a discharge of gaseous fuel from a surface - solid surface or vent with specified heat release rate per unit area HRRPUA applying prescribed kW m^{-2} to a given surface or mass loss rate of fuel gas per unit area MLRPUA applying $\text{kg m}^{-2} \text{s}^{-1}$. For more realistic fire evolution a time history parameters can be prescribed, from which the most used are parameters TAU and RAMP. TAU_T and RAMP_T controls the rump-up of the surface temperature while TAU_Q and RAMP_Q adjust the heat release rate. The whole list of possible functions for altering the fire evolution is included in a table in [10] For certain fire models specifying the gas burner only is not sufficient as it does not simulate the fire spreading. FDS offers a possibility of definition of a fire spread rate directly without a need to obtain material properties, model the ignition and spread of fire. The fire starts at the defined XYZ point with a spread rate SPREAD_RATE specified by the user in m s^{-1} . It is possible to include time history parameters discussed above with an option that the rump-up of HRR starts after the fire reaches specified point. See the example at [10]

By defining the pyrolysis rate only by one of the options discussed above the combustible (for example a surface of a object, on which is the discharge of gaseous fuel prescribed) doesn't burn away, however it is possible to mimic the burning away of the solid or liquid fuel by using the function BURN_AWAY. If more comprehensive data regarding objects' characteristics² are available, It is possible to define the objects with properties stated above (via MATL and via SURF). By that we are basically saying to FDS that we are controlling the burning rate ourselves but we still want to simulate the heating up and obtain the time when the ignition temperature is achieved. [10]

²Bulk thermal properties, ignition temperature, and subsequent burning rate as a function of time from ignition.

The course of the thermal decomposition can be described by dozens of parallel and subsequent decomposition reactions, however this concept is so complex due to increasing number of specified parameters that there is an effort to simplify the whole process. It is necessary to find and choose such a decomposition reaction scheme containing the less components and reactive reactions possible so that description of thermal decomposition is maintained both qualitatively and a quantitatively. Parameters for assembling the complex pyrolysis model are obtained from direct measurements or from calculations based on experimentally measured data. More of this topic is stated in Salek's diploma thesis [21].

Once a pyrolysis process is realized, gaseous fuels are released from specified surfaces into the compartment. In reality there can be many combustible gaseous fuels present at the burning process, however the simulation in FDS enable to use only one type of gaseous fuel as a surrogate for all potential fuels. That simplification has been implemented due to computational cost of solving transport equations for multiple gaseous fuels. [10]

Chemistry of the modeled burning gaseous fuel should be set to correspond as much as possible to an actual predominant burning gaseous fuel. Setting of the fuel FUEL is done within the command REAC - for FDS 6 this definition is required. FDS provides two ways of specifying the fuel. The simplest way is to choose built-in fuels (such as propane), which has all the needed characteristic for computing set within the FDS database. All the available species are listed in Table 15.1 of FDS User Guide [10]. The other approach allows the user to define the fuel and its components' mass fractions directly by FORMULA, while more specific chemistry details need to be defined. See [10] for additional information.

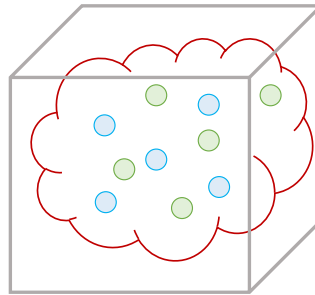


Figure 16: Grid cell. According to author's imagination.

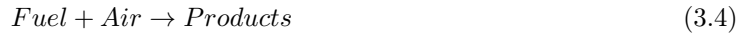
Each grid cell is though of as a turbulent batch reactor. At the beginning of each time step an initial concentration of species is present at a certain degree of mixing. The rate of following mixing process of the species altogether is controlled by turbulence. Once the mixing is complete, the species react. The reaction of fuel and oxygen can react with two possible kinetic parameters:

1. *Mixing-controlled combustion* or *infinitely fast chemistry*, which assumes that reaction of fuel and oxygen is infinitely fast, controlled only by species concentrations. This approach is set by

default.

2. *Finite-rate combustion*, sometimes referred to as *Arrhenius reaction*, is where all the individual gas species are defined and track individually and a very fine grid resolution is required. Thus this approach is costly and is not going to be used or discussed within this thesis.

When a mixing-controlled combustion model is used, three lumped species are assumed: *air*, *fuel* and *products*. And a simple chemical reaction with these 3 lumped species is being considered:



Lumped species represents a mixture of primitive gas species that are grouped and they transport and react together. The typical example of such is the air (mixture of nitrogen, oxygen, carbon dioxide and water vapor) which is in FDS set as a default background if not specified differently. This simplified approach is necessary in order to make the simulation easy to control so from the numerical point of view it is counted with only one species instead of many. If needed, the lumped species mass fractions are determined by primitive species mass fractions Y_α so the primitive species can be recovered from the lumped species just by matrix multiplication. [9]

Then the determination whether the burning occurs depends on whether the temperature and oxygen an fuel ratio are appropriate withing the grid cell. Each cell represents a turbulent batch reactor at a given degree of mixing. This assessment is done for each cell separately - that basically means that in some grid cells burning might occur (for example within those with temperature high enough to ignite the fire) and for those with lower temperature burning won't occur in the given time step.

Flames can be extinguished due to lowered temperatures and dilution of the fuel or oxygen supply. FDS predicts local extinction based on species concentration within the grid cell and the mean cell temperature. Basically there must be sufficient oxygen and fuel to raise the cell temperature from its current value to a *critical flame temperature*. The determination if a self-extinction of fire occurs can be done by two different approaches, both based on critical flame temperature. Critical flame temperature is based on limiting oxygen index LOI which is the oxygen volume fraction at the point of flame extinction and default values for some fuels are stated in FDS User Guide [10].

FDS have implemented two extinction sub-models. One is based solely on oxygen concentration in the grid cell, so called EXTINCTION 1.

The first constraint within this sub-model considers limiting oxygen mass fraction. A limiting oxygen mass fraction is determined as a function of the cell bulk temperature T_{ijk} . This temperature is compared to cut-off temperature T_{cut} .

Cut-off temperature is a weighed average of critical flame temperature T_{OI} and $600\text{ }^{\circ}\text{C}$ ³, and is needed for simulations in which the characteristic grid cell size is much bigger than 1 cm. That is because the combustion occurs only within a fraction of the cell and thus its energy is not sufficient enough to raise the cell's bulk temperature to the critical flame temperature. The second constraint concerns the HRR. Extinction is assumed when potential heat release rate per unit volume of the grid cell is smaller than value dependent on cell's volume, critical flame temperature T_{OI} and temperature of the cell T_{ijk} . [9]

The second extinction sub-model called EXTINCTION 2 is used for grid cell size 1 cm and less. This model considers mass fractions of both oxygen and the fuel within the grid cell. If the potential heat release (rate per unit volume) from the reactants located in the grid cell can not raise the temperature above the critical flame temperature T_{CFT} , the combustion is suppressed. This model assumes that excess of fuel within the cell acts like a diluent. The opposite is assumed with an excess of air and proportional amount of products. So it is more likely that burning occurs in bigger cell which is mostly consisted of air with small amount of fuel rather than in a cell mostly filled with fuel.[9]

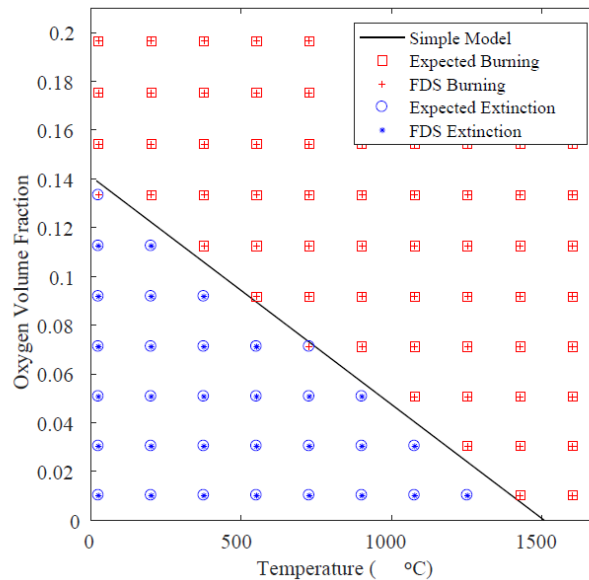


Figure 17: Viability of combustion for an array of initial temperatures and oxygen concentrations. Reprinted from [10].

It is observed that FDS predictions based on the EXTINCTION 2 model (red crosses for sustainable burning, blue stars for extinction) correspond with the expected results using thermophysical properties of the reactants and products. The simplified linear model, EXTINCTION 1, comply with the more detailed calculation. More detailed information on the extinction model can be found in the FDS Technical Reference Guide. [9]

³It is the temperature at which the unburnt fuel and oxygen mix and burn within the hot gas layer. The particular value $600\text{ }^{\circ}\text{C}$ is based on two measurements (of Pitts and Bundy), which have shown that the O_2 concentration drops to 0 when the temperature increases above $600\text{ }^{\circ}\text{C}$.

3.3.2 Outputs

The heat release rate from the combustion is being calculated by summing the lumped species mass production rates times their respective heats of formation [9]:

$$\dot{q}''' = - \sum_{\alpha} \dot{m}_{\alpha}''' \cdot \Delta h_{f,\alpha} , \quad (3.5)$$

where

- \dot{q}''' is heat release rate per unit volume,
- \dot{m}_{α}''' is mass production rate of the lumped species α ,
- $\Delta h_{f,\alpha}$ is heat of formation of the lumped species α .

The mean cell gas temperature is calculated from equation [9]:

$$T_{ijk} = \frac{\bar{p}_m}{\rho_{ijk} \cdot R \cdot \sum_{\alpha=0}^{N_s} (Z_{\alpha,ijk} / W_{\alpha})} , \quad (3.6)$$

where

- T_{ijk} is temperature of ijk -cell,
- \bar{p}_m is background pressure of m th pressure zone,
- ρ_{ijk} is density of cell ijk ,
- R is universal gas constant,
- $Z_{\alpha,ijk}$ is species mixture α of cell ijk ,
- W_{α} is molecular weight of gas species α .

It is necessary to distinguish between the ideas of computing rate of heat release and the temperature. Heat release rate is being calculated for the whole volume of the examined enclosure. In contrast, the gas temperature is being calculated for each computational cell separately.

Part II

Analysis of Input Parameters for Numerical Fire Simulations

4. Analysis of Input Parameters

An analysis of the extent of the ventilation influence to temperature and energy progress within a compartment was conducted. Three mathematical models were considered. Parametric fire curve from Eurocode 1991-1-2, considering the compartment to be one volume only. Zone model based software CFAST dividing the compartment into two volumes horizontally, calculating the temperature progress for each separately. The last applied fire model is a computational fluid dynamics based software FDS, which discretizes the space into a specified number of elements.

4.1 Compartment

A representative compartment was developed for examination in three fire models. For an uncomplicated imagination a very simple floor plan of a rather small office was assumed¹.

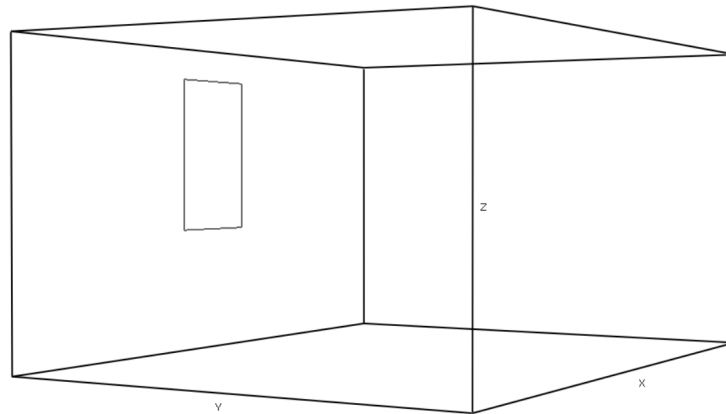


Figure 18: Geometry of the analysed compartment.

The office inner dimensions are 6.0 x 4.5 x 3 m. The dimensions correspond to coordinate axis x , y and z which are indicated in the figure above. The compartment contains an only ventilation opening at the rear size of compartment facing to outside. The window width is the examined value in the following analysis. Thus, the dimension of the window width in Figure 18 is only illustrative. However, the height of the window remains constant throughout the whole research for each fire model and has been set to be 1.5 m with a sill of 1.2 m.

A floor plan with the indication of inner dimension of the examined enclosure are illustrated in Figure 19. The window width is a subject of examination and will be referred to as w throughout the whole analysis.

¹Any resemblance to office of supervisor of this thesis is purely coincidental

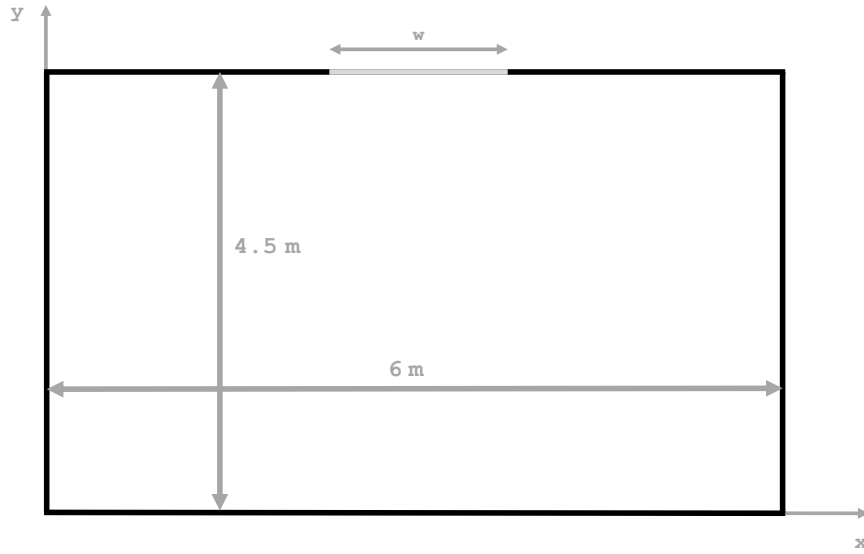


Figure 19: Floor plan of analysed compartment with indicated dimensions.

The window height is set to be constant during the whole analysis. This choice was made in order to prevent any side-influences to the heat release rate progresses and the burning regime assumption within the fire model. As discussed in section 2.3.2, the burning regime is closely related to so-called ventilation factor, which does not only depends on the opening area, but at its height as well.

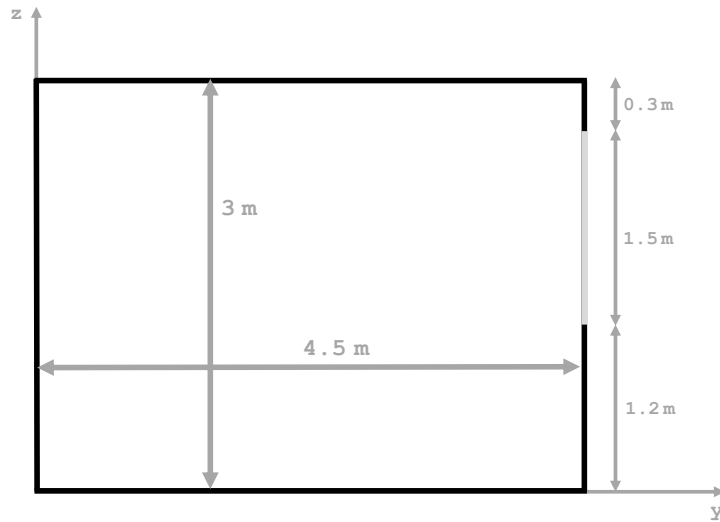


Figure 20: Cross-section of analysed compartment with indicated dimensions.

The surroundings constructions, surrounding walls, floor and ceiling constructions, are all assumed to be 0.3-m-thick. The material of the constructions is a concrete of common characteristics, which are given in Table 1. The material characteristics are assumed to be independent on the rising temperature, thus remain constant during the whole duration of the fire simulation.

Table 1: Window widths with corresponding value of maximum HRR

| | Density kg/m^3 | Conductivity W/mK | Specific Heat J/kgK |
|----------|------------------|---------------------|-----------------------|
| Concrete | 2300 | 2 | 900 |

4.2 Energy Input

For all three fire models an energy input from Eurocode 1991-1-2 is assumed. 80 % fractile of fire load density from Table E.4 for occupancy *office* is considered for the parametric fire curve model. For the zone model and computational fluid dynamics model the fire load density is a insufficient input. A rate, on which the energy is being evolved and maximum rate of heat release must be defined as well and are taken from Table E.5. This prescription is called t-squared fire curve and its definition and more details are included in section 2.3.1.

4.3 Parametric Curve Analysis

For the purposes of the analysis a parametric fire curve was implemented and plotted in mathematical software MATLAB [18].

In principle, parametric fire curve distinguishes between fuel-controlled and ventilation-controlled fire. For each situation a different relation is being used depending on the size of the value O . Value O is determined from the size of the opening area and thus is directly influenced by. So to determine the point of burning regime switch a calculation of the parametric curve was conducted for different values of the window width and consequently, different opening factors O .

A loop cycle has been developed, plotting the curves depending on what kind of relation has been used to determine its progress and thus the burning regime. For an illustration parametric curves for ventilation factor within their range of usability ² to demonstrate its functionality are plotted in Figure 14.

To stay within the limits of opening factor O , the window widths in investigated compartment were chosen to vary between $w = 1.5$ m and $w = 5.0$ m with 0.5 m step and are plotted in Figure 21.

All outputs were compared to parametric fire curves plotted by FMC [17] software to assess the validity of the results, which has been confirmed.

²Within the limit values 0.02; 0.2

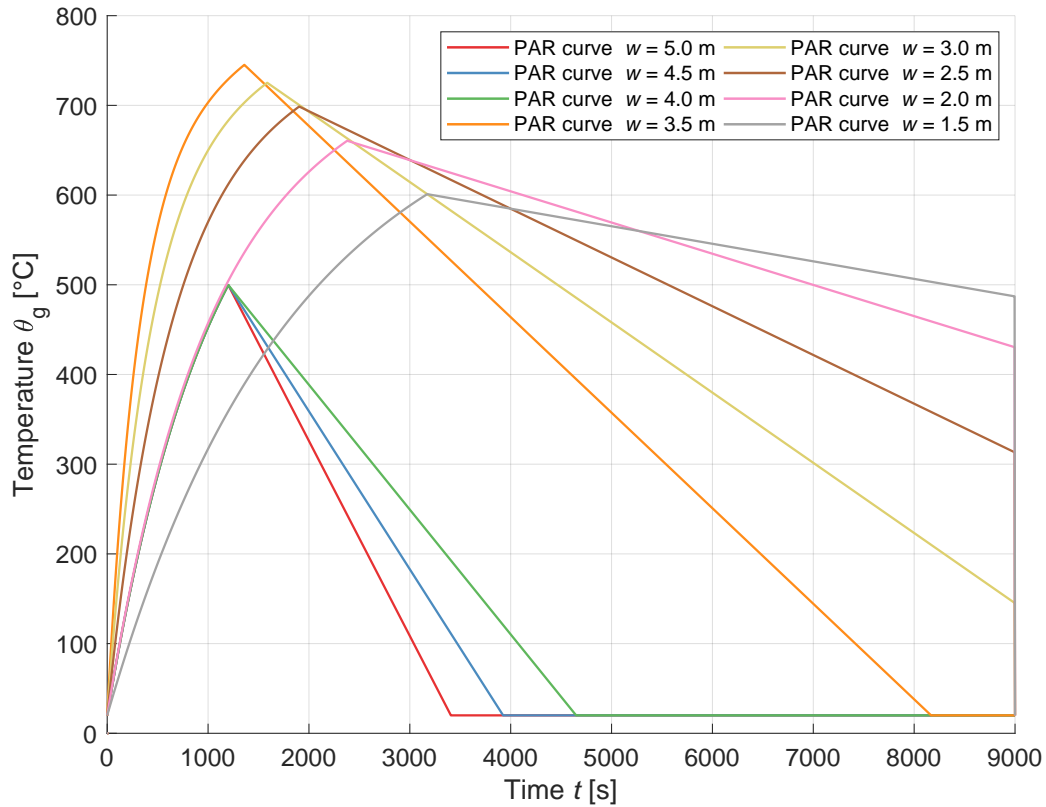


Figure 21: Illustration of parametric curve progresses assuming window width $w = \langle 1.5; 5 \rangle$ m with step of 0.5 m.

A gap between curves, which are determined by relation valid for fire controlled by fuel and the curves calculated from relation valid for ventilation-controlled fire, is observed. The peaks of ventilation-controlled parametric curves are reaching 550–750°C in the contrast with the peak of all fuel-controlled fire curves, which reach 500°C.

The idea behind above presented curve progresses is that when the fire has a window of such a size providing sufficient oxygen amount, it also means that there is enough opening area to discharge the hot gases from the compartment outside of it.

Two particular parametric curves located right at the switch of the burning regimes were determined and are plotted in figures below. As the step was chosen to be 0.5 m, the point of changing the burning regime from ventilation-controlled to fuel-controlled is located between the window widths 3.5 m and 4.0 m.

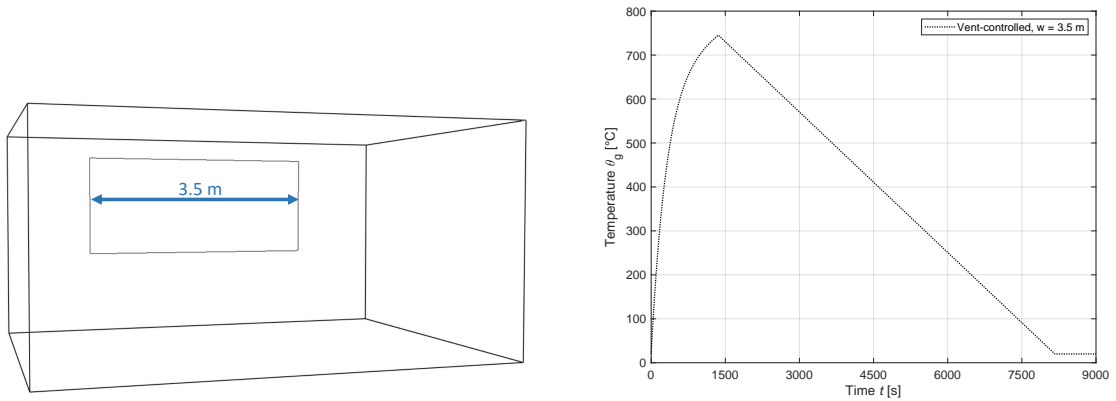


Figure 22: Parametric fire curve progress assuming window width 3.5 m.

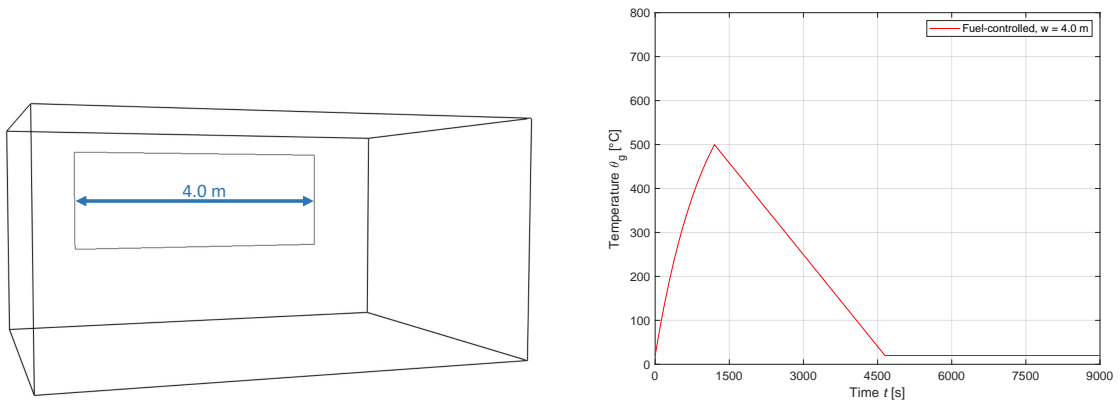


Figure 23: Parametric fire curve progress assuming window width 4.0 m.

In Figures 22 and 23 the difference between the temperatures for a rather small difference in the opening width is emphasized.

For a change in window width of 0.5 m, or 0.075 m^2 , the parametric curve model assumes a 250-degree difference in the temperature progress. As the parametric curve is being used mostly for design of construction at fire situation, the slight difference in the opening area could be crucial for following design and assumptions.

4.4 Zone Model CFAST

An examination of temperature and energy progresses in compartment described in part 4.1 was conducted in zone model based software CFAST [11]. First, information about the energy input is included. The following part is dedicated to comparison of the heat released rate defined by user and heat released rate calculated by the software. Then the temperatures of both upper and lower layer

are compared to temperatures progresses from previous fire model, the parametric fire curve.

4.4.1 Energy Input

The fire is assumed to have a form of a fire plume placed in the centre of the compartment $x = 3$ m, $y = 2.25$ m. The rate of heat released is mimicked by t-squared fire, which determines the rate of energy of present combustible material evolved during the fire situation, depending on the occupancy of the compartment (see section 2.3.1).

One of the option of defining a fire is to specify t-squared fire directly. Specifically, the maximum heat release rate and the duration of the growth phase, steady burning period and decay phase need to be specified. The fire growth rate can be chosen between *slow*, *medium*, *fast* and *ultra-fast*, whose values correspond to 600, 300, 150 and 75 s as stated in Table E.5 of Eurocode 1991-1-2 [8].

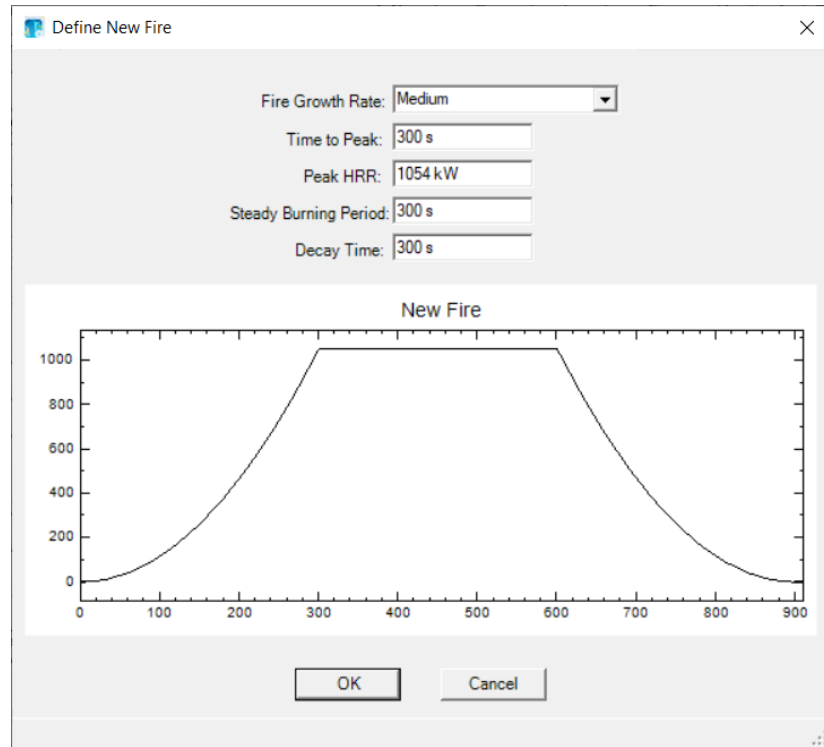


Figure 24: Defining a fire by t-squared curve in CFAST.

For the purposes of the analysis a MATLAB [18] code was developed to determine the progress and values needed as an input to CFAST. The process of t-squared curve definition was consisted of three simple steps:

1. Setting of a window area (window height remains the same) in CFAST simulation,
2. determining the progress of a t-squared fire - more specifically the duration time of each phase and maximum rate of heat release (and thus position of the horizontal plateau),

3. description of a fire within CFAST, by a direct t-squared fire definition which demands inserting the above mentioned inputs.

T-squared fire curves, which were used as the inputs to CFAST simulation, are plotted in Figure 25.

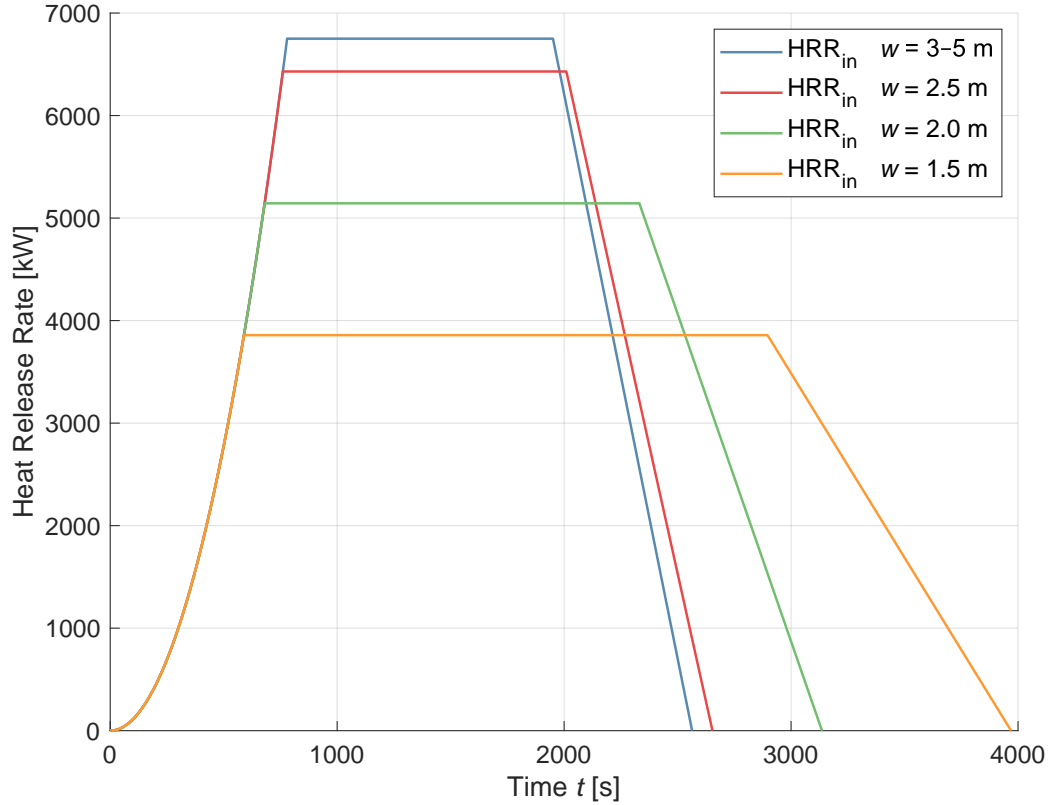


Figure 25: Comparison of t-squared fire curves assuming different window widths, used as HRR inputs for CFAST.

Rather bigger changes in the rate of heat release progresses can be observed while only window widths are being diversified. For window widths $\langle 3; 3.5; 4; 4.5; 5 \rangle$ m the model presumes that the window area is large enough to provide the fire with enough amount of oxygen. For window widths lower than 3 m there is a restriction of maximum amount of rate of heat release due to lack of oxygen and the curve is then prolonged adequately to maintain the energy released. That restriction is made by simplified equation 2.2 given by Eurocode 1991-1-2 [8]. The maximum values of each t-squared curve are included in Table 3 in following chapter.

The difference in assumption of burning regimes for the parametric fire curve and the t-squared fire curve (t^2) are given in Table 2.

Table 2: Comparison of burning regime assumptions using the parametric fire curve and the t-squared fire curve.

| Burning Regime | Parametric Curve | t^2 |
|----------------|------------------|-----------------|
| 0.5 | Vent-Controlled | Vent-Controlled |
| 1.0 | Vent-Controlled | Vent-Controlled |
| 1.5 | Vent-Controlled | Vent-Controlled |
| 2.0 | Vent-Controlled | Vent-Controlled |
| 2.5 | Vent-Controlled | Vent-Controlled |
| 3.0 | Vent-Controlled | Fuel-Controlled |
| 3.5 | Vent-Controlled | Fuel-Controlled |
| 4.0 | Fuel-Controlled | Fuel-Controlled |
| 4.5 | Fuel-Controlled | Fuel-Controlled |
| 5.0 | Fuel-Controlled | Fuel-Controlled |

4.4.2 Energy Outputs

One of the calculated values in CFAST simulation is the heat release rate from equation 3.2. By this relation CFAST determines if the fire has enough oxygen or if needs to be restricted accordingly. The calculated heat release rates from the simulations were compared to input t-squared fire curves to assess if a restriction by the program has been made.

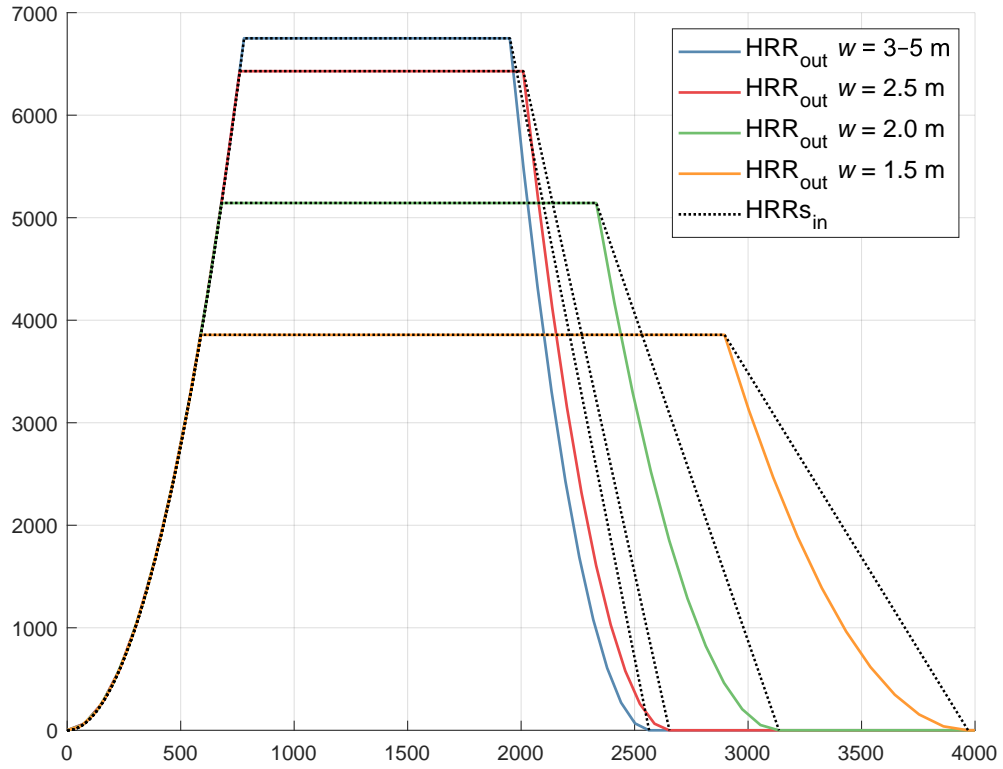


Figure 26: Comparison of input HRRs (t -squared fire curves) and HRR outputs.

It is observed that the growth phases and horizontal plateaus of input HRR and output HRR are equal. The only differences spotted are among the decay phases - CFAST is assuming the decay phase to have parabolic progress unlike Eurocode [8] which defines the decay as a linear line.

It can be seen that there is no restriction of maximum value of heat release rate by CFAST. That means that the assumption about the availability of oxygen by equation 2.2 is more restrictive than the assumption 3.2 implemented in CFAST.

However, as stated in [8] there are two options of determining whether the fire abounds with enough amount of oxygen or needs to be reduced following the available oxygen content. The first and already demonstrated approach is to use simplified equation 2.2. The second option is to conduct the assessment automatically in zone model based software.

As a demonstration of how the reduction assumption in zone model is being approached, a simulation was conducted. The maximum value of heat release rate (such for 5-m-wide window) was considered as an input energy of the fire. In the simulation a window width of only 1 m was modelled.

In Figure 27 the t -squared fire for 5 m wide window, used as an input, is plotted altogether with heat release rate calculated by the software, when considering 1-m-wide window. A t -squared fire

curve for window width of 1 m is also included for comparison.

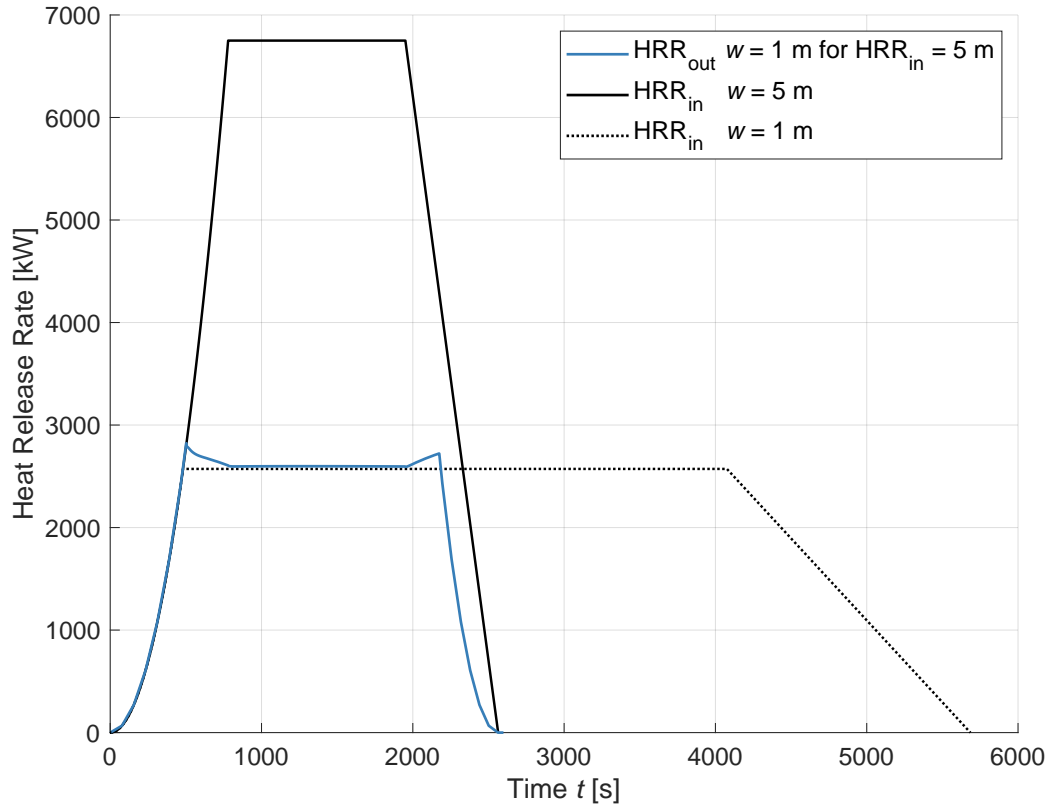


Figure 27: Demonstration of CFAST inputs limitation due to insufficient oxygen availability. T-squared fire curves denoted as HRR_{in} for window widths 1 and 5 m are compared to HRR output from zone model based CFAST simulation with 1-m-wide window with energy input for 5 m.

As observed, the CFAST heat release rate output is restricted due to insufficient access of oxygen. However the curve is not prolonged and thus the overall energy is not maintained. CFAST calculation is following the prescribed rate of energy evolution, reducing only the part with insufficient amount of oxygen. The reduced value of maximum heat release rate from CFAST corresponds to its counterpart value determined by the simplified equation from Eurocode [8].

Even though that the reduced value of maximum heat release rate from zone model corresponds to the reduction made by simplified relation from Eurocode, it is necessary to bear in mind, that the algorithm implemented in CFAST doesn't account for the conservation of the energy released during a fire.

Thus, than assessing the reduced value of HRR following the available oxygen content in zone model, it appears to be more sufficient to implement the simplified relation 2.2 directly to the spread sheet or numerical computing environment, where the t-squared curve progressed is being assessed.

4.4.3 Temperature Outputs

An assessment of temperature progresses for varying window widths $<1.5; 5>$ m with 0.5 m step was conducted. The heat release rate inputs (t-squared fire curves) for different window widths are plotted above. Both upper layer temperature and lower layer temperature are compared with temperatures obtained in previous analysis by parametric fire curves.

To preserve a clear representation of output data, comparison of parametric curves and temperature output from CFAST were plotted to separate figures depending on a burning regime assessed by parametric curve.

In Figure 28 a comparison of fuel controlled parametric curves and mean lower temperature from a two-zone model is plotted.

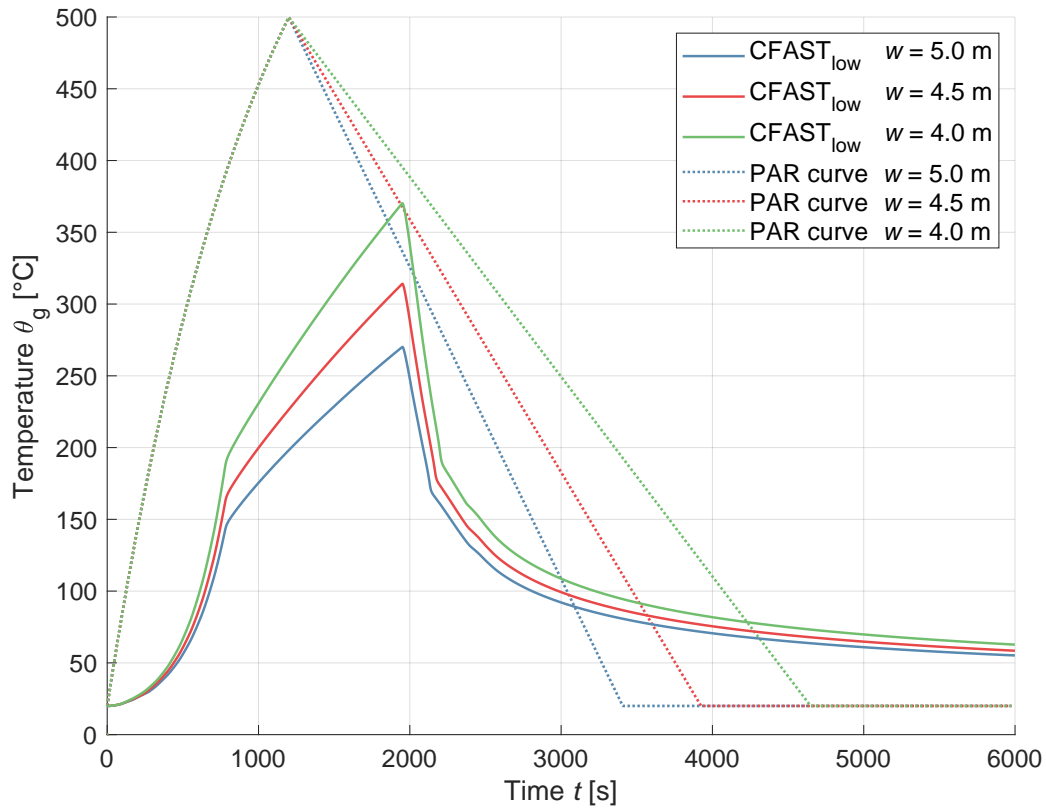


Figure 28: Comparison of lower layer temperature progresses from CFAST and fuel-controlled parametric curves assuming window widths $<4.0, 4.5, 5.0>$ m.

In case of the parametric curves, the maximum temperature reached remains 500 °C. The cooling parts duration differ on a ~ 10 minutes. For the temperatures calculated in zone-model, the maximum temperature is reached in the simulation with 4.0-m-wide window and is 372 °C. While expanding the window width, maximum reached temperatures decays. Particularly for window width 4.0 m the

value is 315 °C, for 5.0 m it is 269 °C. The cooling phases follow the similar progress and do not differ much.

In Figure 29 the parametric curves from Figure 28 are now being compared to mean upper layer temperature from CFAST simulation.

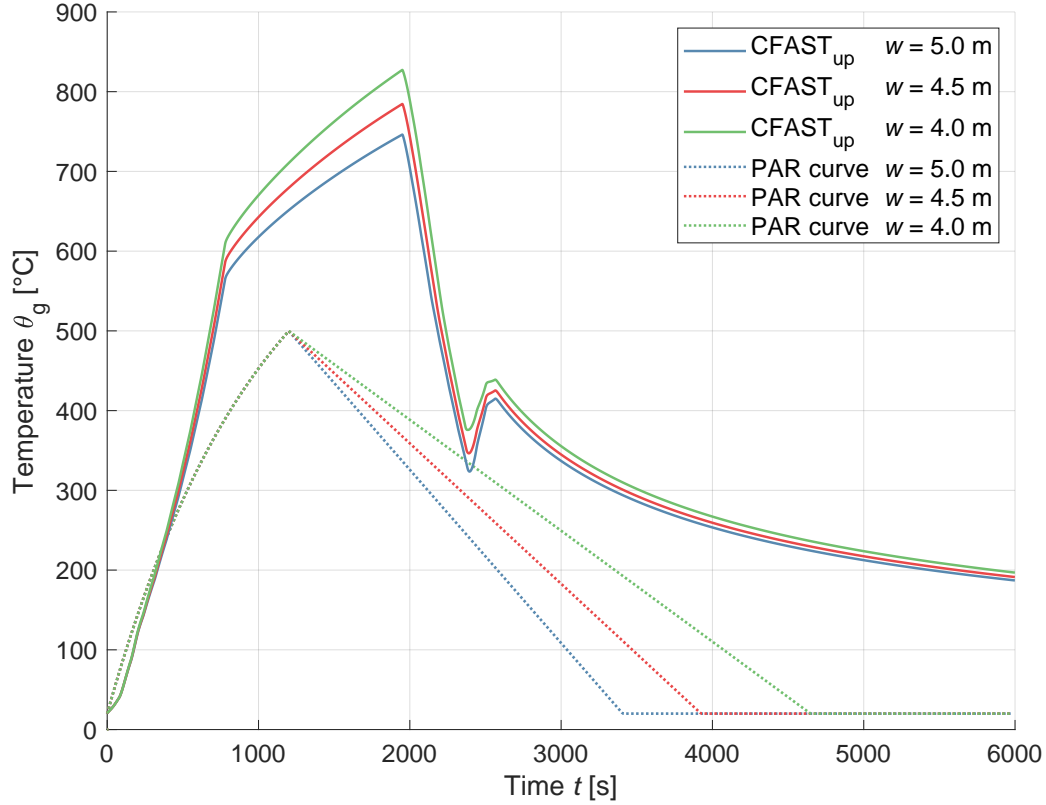


Figure 29: Comparison of upper layer temperature progresses from CFAST and fuel-controlled parametric curves assuming window widths $\langle 4.0, 4.5, 5.0 \rangle$ m.

The upper layer temperature maximums exceed the parametric fire curves values over 250 °C. The highest temperature is reached for window width 4 m, then it slightly decays as seen at previous figure. This seeming paradox is observed due to discharge of hot gases through the opening. The rapid change in a temperature progress corresponds to the time, when t-squared fire curve depletes all the fuel potential.

Similarly, a comparison of parametric curves with a prescription for ventilation-controlled fire with upper and lower layer are included below.

In Figure 30 lower layer temperatures and ventilation-controlled fire curves for window widths $\langle 1.5, 2.0, 2.5, 3.0, 3.5 \rangle$ m are plotted.

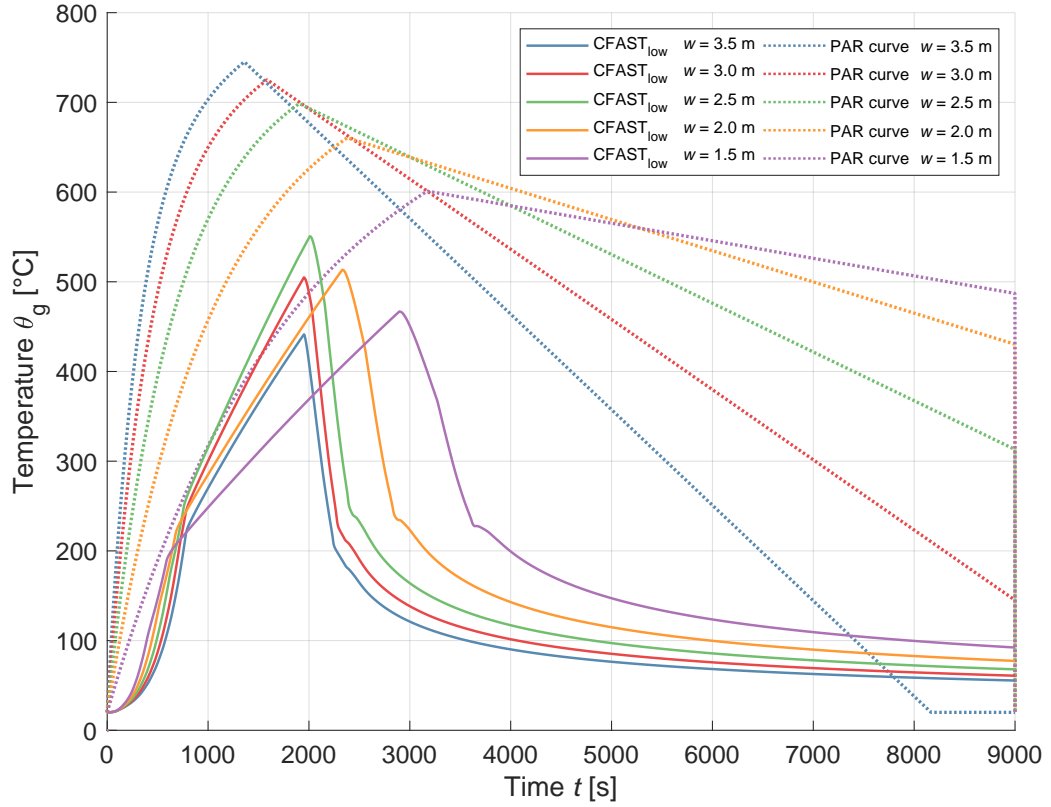


Figure 30: Comparison of lower layer temperature progresses from CFAST and ventilation-controlled parametric curves assuming window widths $\langle 1.5, 2.0, 2.5, 3.0, 3.5 \rangle$ m.

Unlike their fuel-controlled counterparts, ventilation-controlled parametric curves vary in the reached maximum values of temperature. The cooling part is the longer the smaller the window area is. Lower layer temperatures maximums from zone model rises as the window area shrinks. This trend stops at the width of 2.5 m and starts to decay. The cooling part varies more than when considering larger window areas (as in Figure 28). When cooling, for the compartment with window width 3.5 m, the temperature reaches the value of 200 °C at second 2300, while for compartment with 1.5-m-wide window the decay part reaches the temperature at the second 4000.

In Figure 31 the upper layer temperatures and ventilation-controlled fire curves for window widths $\langle 1.5, 2.0, 2.5, 3.0, 3.5 \rangle$ m are plotted.

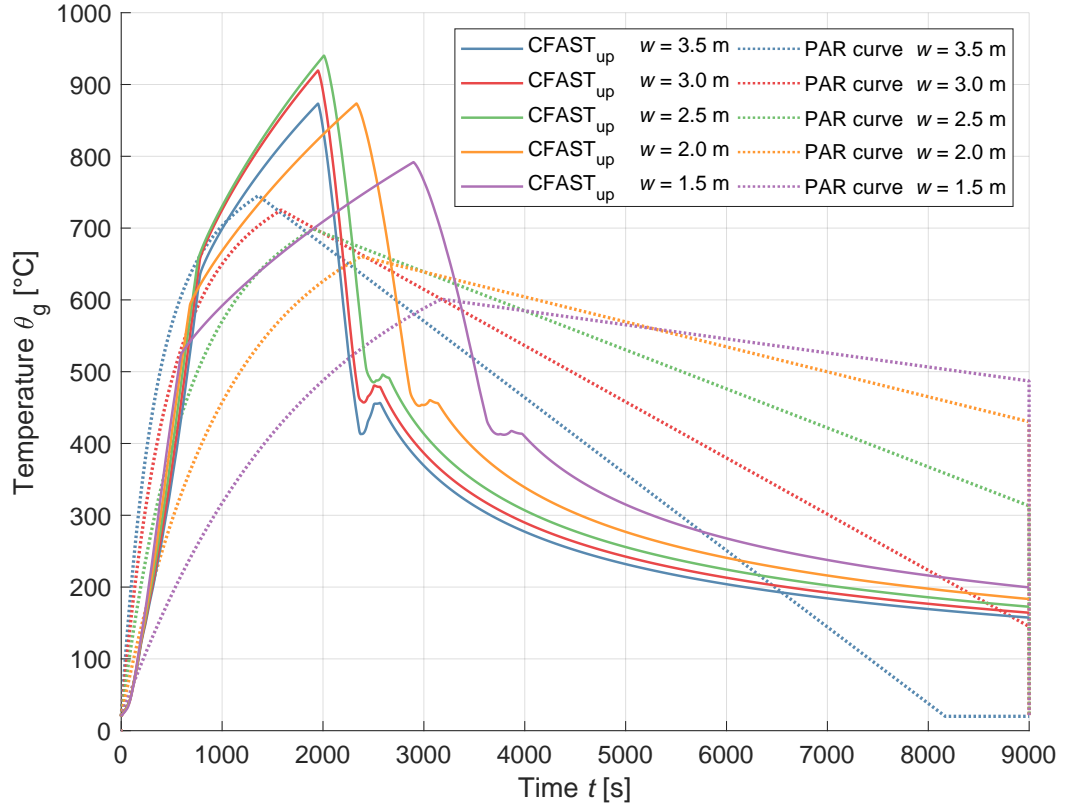


Figure 31: Comparison of temperature progresses from CFAST and ventilation-controlled parametric curves assuming window widths $\langle 1.5, 2.0, 2.5, 3.0, 3.5 \rangle$ m.

The trend of the maximum values reached within the upper layer copies the trend observed in the maximum values of the lower layer. The maximum temperatures increase as the window area is getting smaller. After reaching window width 2.5 m, the maximums start to decay. The deviation from the progress of the cooling part are observed at the times of the considered depletion of fuel by t-squared curve.

For an illustration a weighted mean average temperature was computed based on the layers' heights. The lower layer heights are plotted in Figure 32. The axis called Smoke Layer Height can be thought as of axis z of the compartment.

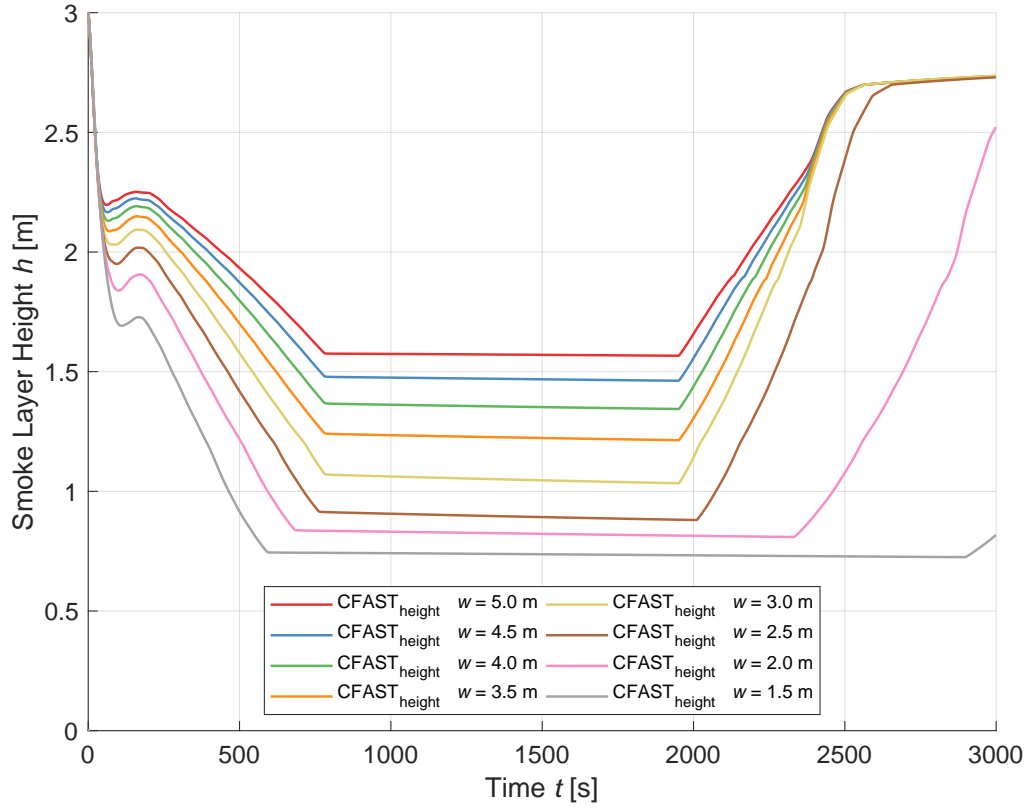


Figure 32: Smoke layer's lower surface height.

Then the mean average temperature within the compartment was calculated from Equation 4.1.

$$\bar{t} = \frac{t_U \cdot h_U + t_L \cdot h_L}{h_U + h_L}, \quad (4.1)$$

where

- \bar{t} is a weighted arithmetic mean temperature [$^{\circ}\text{C}$],
- t_U and t_L is temperature of upper respective lower layer [$^{\circ}\text{C}$],
- h_U and h_L is height of upper respective lower layer [m].

Lower layer height is one of the outputs from the simulation, upper layer height was taken to be an addition to compartment's inner height, which is 3 m.

Fuel-controlled parametric curves for window widths <4 ; 4.5 ; 5 m are compared to the mean average temperatures calculated from equation above and are plotted in Figure 33.

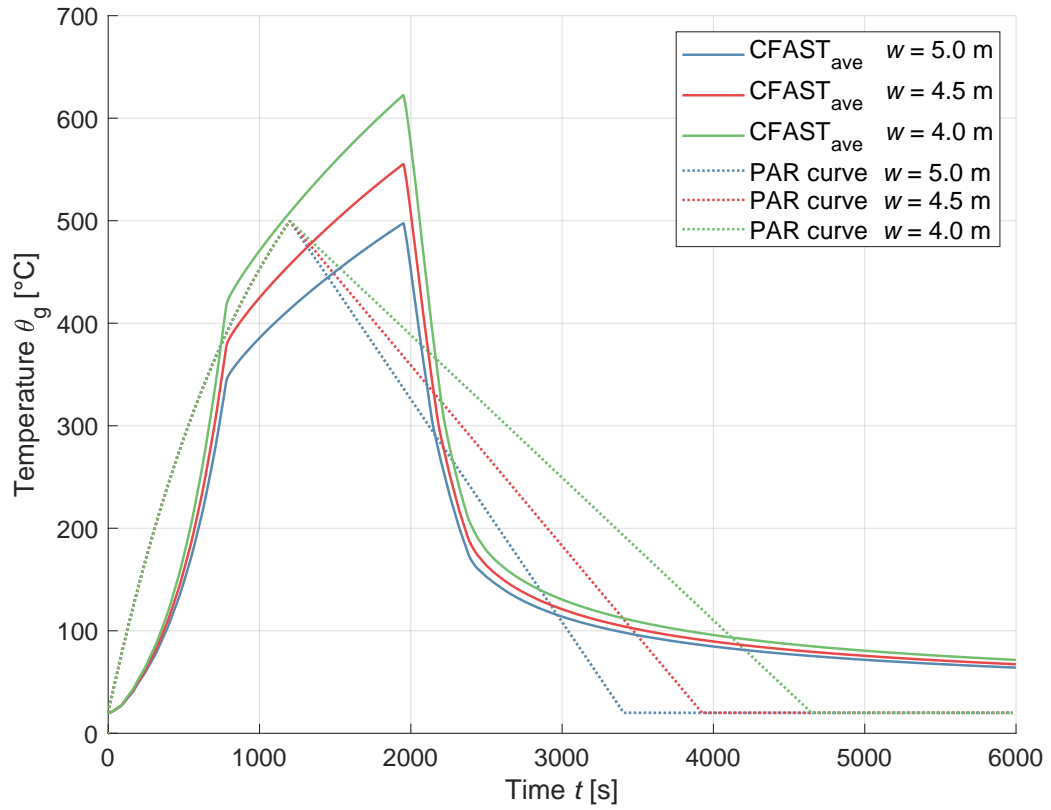


Figure 33: Comparison of mean average temperature progresses from CFAST and fuel-controlled parametric curves assuming window widths $\langle 4.0, 4.5, 5.0 \rangle$ m.

Parametric curve maximum temperatures are reached in the order of minutes sooner and the cooling part is more gradual. In contrast the maximum temperatures from CFAST are reached later, followed-up by a steep decline which gets more gradual progress after the fuel depletion.

The ventilation-controlled parametric curves and mean average temperatures for window widths $\langle 1.5, 2.0, 2.5, 3.0, 3.5 \rangle$ m are plotted in Figure 34.

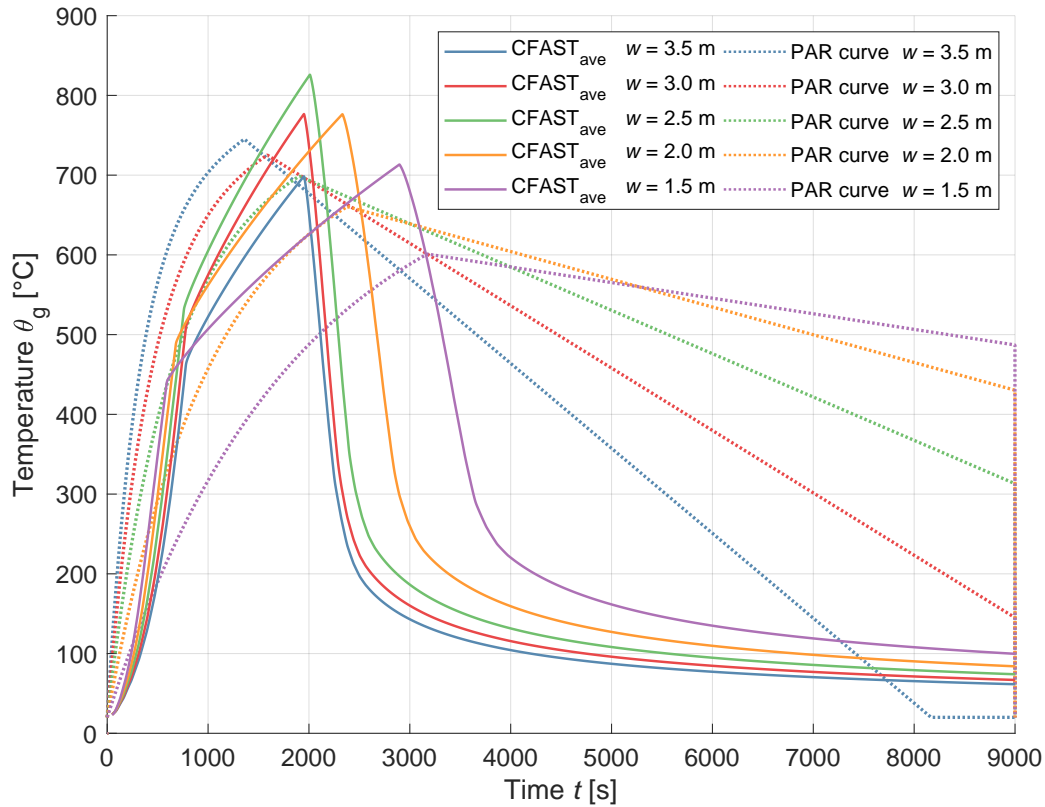


Figure 34: Comparison of mean average temperature progresses from CFAST and fuel-controlled parametric curves assuming window widths $\langle 1.5, 2.0, 2.5, 3.0, 3.5 \rangle$ m.

The parametric curve progresses, which are controlled by ventilation, are more alike to average temperatures from zone model. The main difference lies in the cooling part - the temperature outputs from CFAST are more steep right after reaching the maximum temperature, as following the prescribed t-squared curve, then get more gradual. Parametric curves' cooling part gets the longer and more gradual as the opening area shrinks.

It must be emphasized, that the temperature outputs from zone model CFAST have been averaged from upper and lower layer temperatures just for illustration and purposes of this thesis. While developing a structural fire design, the temperature considered is closely related to the type of structure which is being analysed and its location.

4.5 Fire Dynamics Simulator

A sensitivity analysis is conducted in a computational fluid dynamics based software FDS [22]. A rather small room, an office described in part 4.1 is modelled. First, information regarding distribution of the compartment's volume into definite number of elements and ventilation and energy consideration

is included. Similarly as in the previous chapter, an extent of ventilation influence to HRR and temperature progresses are analysed. Then a different chemical compounds input are considered to take part within the process of combustion, and the heat released rates and temperatures are compared.

4.5.1 Compartment Geometry and Mesh

The numerical analysis is conducted in office of a size $6.0 \times 4.5 \times 3$ m. The general geometry of the compartment is demonstrated in Figure 36, where a simulation of a fire at its 1000 seconds is shown.

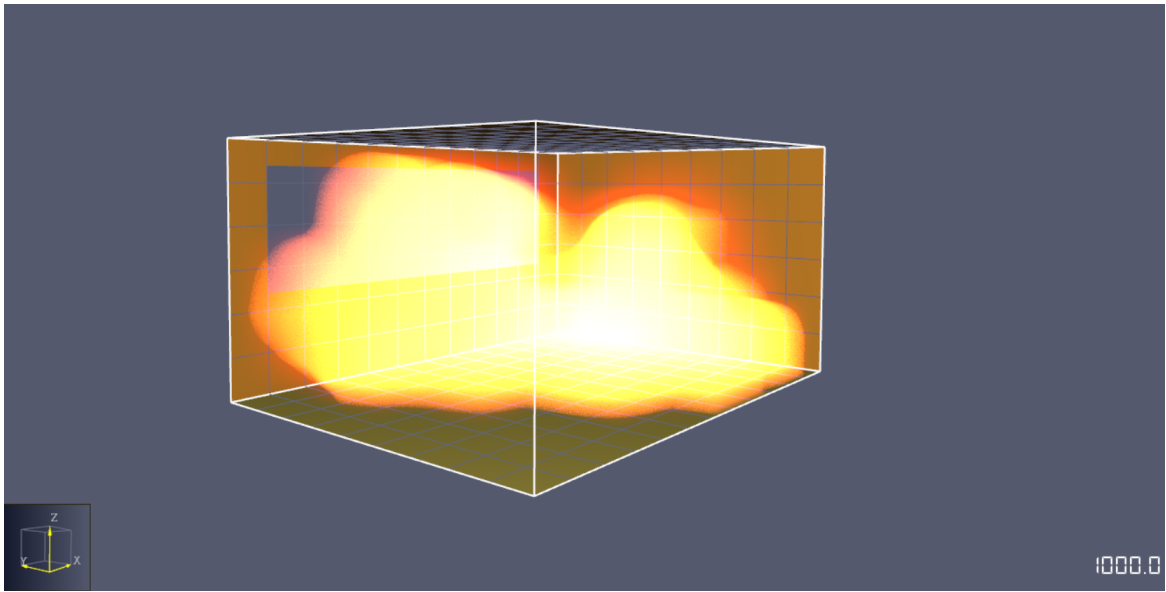


Figure 35: Fire simulation at its 1000th second when the fire is fully developed. Screenshot by author.

The most challenging topic within FDS is the mesh size assessment. The problem is computational cost when the mesh is too fine. The author has used a mesh size calculator [2] to determine a proper mesh for this particular analysis. Three types of meshes were offered. Coarse mesh compounded of 0.5-m-long-edge cubes, moderate with 0.2-m-long-edge cubes and fine mesh of cubes of edges 0.1 m long.

Mostly due to computational time savings a coarse mesh was chosen. The compartment was divided into 12, 9 and 6 pieces for axis x , y and z . Hereby a mesh of cubes with an edge of 0.5 m was developed. The total number of cells is thus 648.

4.5.2 Ventilation

Window height of 1.5 m is preserved for all simulations not to influence the exhaust of the hot gases by changing the window height and thus position of the window (see chapter 2.3.2). When a different

window areas are desired within the simulation, the window width is being changed as shown in Figure 36. The centre axis of the window remain stable to maintain the symmetry of the opening in relation to the compartment geometry.

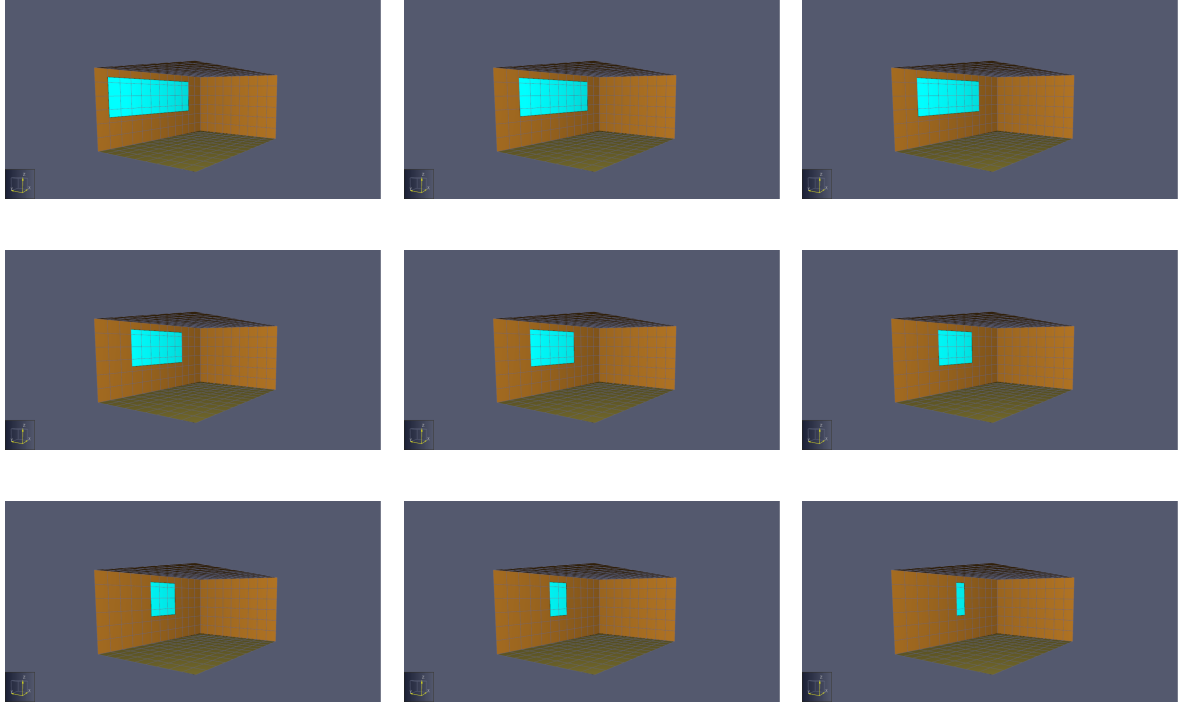


Figure 36: Compartment geometry with different opening areas. Screenshots by author.

4.5.3 Energy Input

The process of pyrolysis is defined by a gas burner placed on the floor of the compartment with prescribed heat release rate. For more details, and options of pyrolysis definition are stated in section 3.3.1.

The process of assessing the progress of heat release rate from the gas burner placed on the floor was set from 3 steps:

1. Setting of the window width for the particular simulation,
2. assessment of a t-squared fire curve progress based on [8] for the specific window width,
3. application of the t-squared fire as an prescribed heat release rate of a gas burner defined within SURF function (see section 3.3.1).

The particular progresses of t-squared curve while considering window widths $\langle 0.5 : 0.5 : 5 \rangle$ m are plotted in Figure 37.

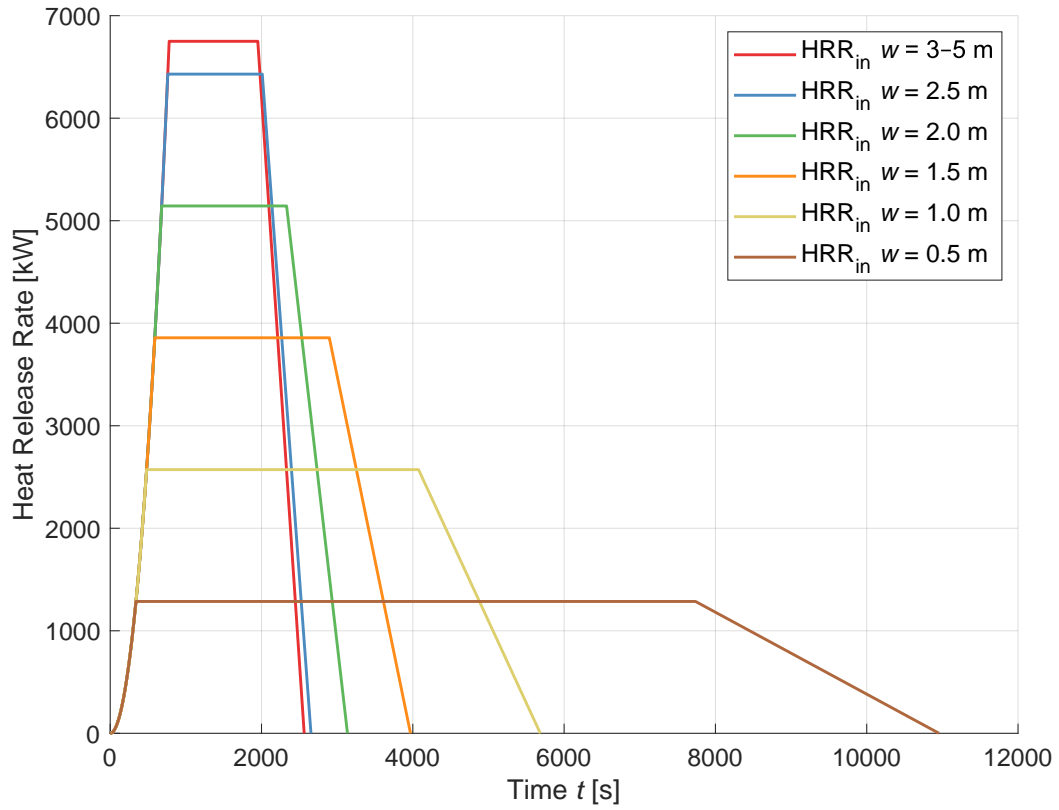


Figure 37: T-squared fire curves progresses used as input rates of heat release for different window widths within FDS simulation.

A table with the particular maximum values of the rates of heat release are included below. If the maximum value of heat release rate is not restricted, the curve is being referred to as fuel-controlled. If the maximum HRR is restricted due to simplified equation 2.2, the burning regime governing t-squared fire curve is said to be ventilation-controlled.

Table 3: Window widths with corresponding value of maximum HRR and burning regime assumption according to Eurocode 1991-1-2.

| Window Width m | Maximum HRR kW | Burning Regime |
|------------------|------------------|-----------------|
| 0.5 | 1286 | Vent-Controlled |
| 1.0 | 2572 | Vent-Controlled |
| 1.5 | 3857 | Vent-Controlled |
| 2.0 | 5144 | Vent-Controlled |
| 2.5 | 6430 | Vent-Controlled |
| 3.0 | 6750 | Fuel-Controlled |
| 3.5 | 6750 | Fuel-Controlled |
| 4.0 | 6750 | Fuel-Controlled |
| 4.5 | 6750 | Fuel-Controlled |
| 5.0 | 6750 | Fuel-Controlled |

As clearly presented in the table, the fire is not limited and reaches the maximum HRR, and is thus fuel-controlled, when the opening has width equal to or more than 3 m. As the window width gets smaller, the maximum heat release rate is restricted and the whole curve is prolonged equally as stated in section 2.3.1.

The gaseous fuel taking place in combustion process and defined in REAC, was set to be propane, as it is said to be the most comprehensive surrogate fuel to mimic burning of organic combustibles. [28]

4.5.4 Energy Outcome

An analysis of FDS's assumption of an influence of ventilation to a prescribed energy release rate is conducted. Window widths $<0.5 : 0.5 : 5>$ m and the their corresponding energy inputs are the only input data varying while the rest of remain preserved.

The prescribed rates of heat release via t-squared curves (Figure 37 are compared to calculated rate of heat releases from FDS simulation in Figure 38.

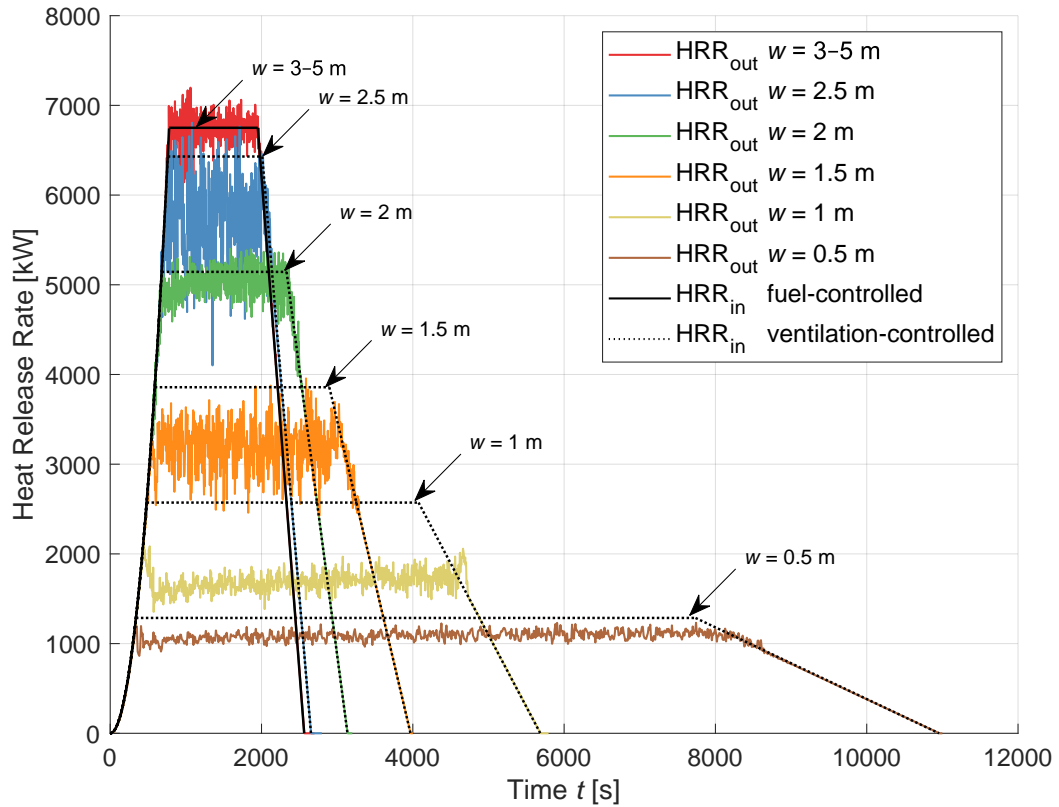


Figure 38: Comparison of HRR inputs (t -squared fire curves) and output HRRs from FDS simulation assuming different opening areas.

For widths $<3; 3,5; 4; 4,5; 5>$ m the t -squared fire curve has the same development. This statement is valid as well for the heat release rates calculated within the simulation. However, if the fire lacks oxygen and starts to be ventilation-controlled, the outcome maximums of heat release rates from FDS simulation are lower than their input counterparts. That means that FDS's extinction sub-model assumes, that the conditions for burning to occur within the grid cell are not fulfilled and consequently unburned fuel is leaving the compartment without the chance to react³.

To demonstrate the oxygen availability assumption more clearly, another simulation was conducted. A fuel-controlled t -squared fire curve (5-m-wide window assumed) was used as an input for the simulation with propane taking place in the combustion process. In the simulation, however, only 1-m-wide window was modelled. The calculated heat release rates progress is plotted in Figure 39. It is compared to unrestricted t -squared fire curve used as an input to the simulation, and t -squared fire curve for $w = 1$ m, which is restricted by simplified relation 2.2 from Eurocode 1991-1-2 [8].

³:(

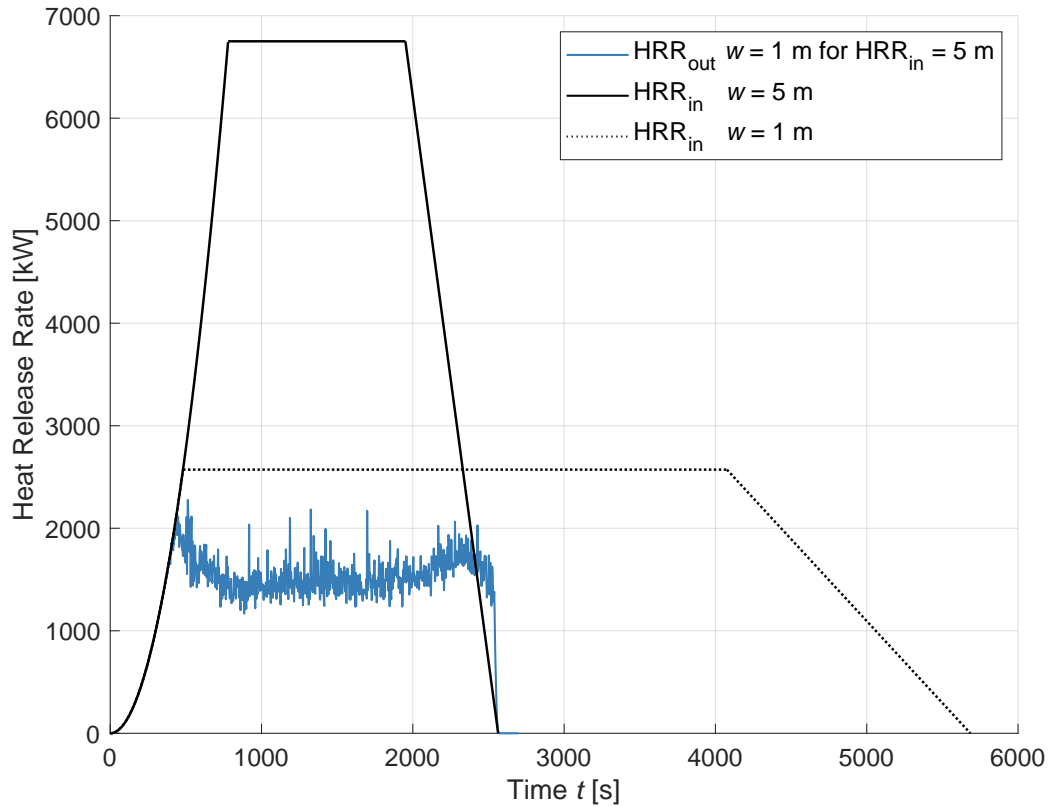


Figure 39: Demonstration of FDS inputs limitation due to insufficient oxygen availability. T-squared fire curves denoted as HRR_{in} for window widths 1 and 5 m are compared to HRR_{out} from FDS simulation with 1-m-wide window with energy input for 5 m.

When using prescribed heat release rate, FDS is using relation 3.6 to assess if the fire is provided with enough oxygen. If the energy prescribed lacks the oxygen to fulfill the prescribed progress, FDS assumes its restriction. However it doesn't maintain the energy released during the fire (mathematically speaking, it doesn't prolong the curve).

Regarding the topic of t-squared fire restriction, as replied by the principal developer of combustion Dr. Jason Floyd in the FDS and Smokeview Discussion [26], the fuel does not burn until it mixes with oxygen under conditions that meet the flammability requirements of the combustion model. If an energy, that is not capable of burning under the ventilation conditions in the model, is prescribed, it will not burn. However, if the exact progress of t-squared fire is desired, there are options, which however require user's intervention to FDS's assumption and default settings, which are based on results from a wide variety of full-scale validation experiments. These are:

- To define a fuel chemistry with an unrealistically high $EPUMO_2^4$ or $HEAT_OF_COMBUSTION$,

⁴It is the amount of energy released per unit mass of oxygen consumed. If the heat of combustion is not explicitly specified, it is calculated by multiplying mass of consumed O_2 with $EPUMO_2$ [10].

- to define a surface with specifying the convective heat flux rather than a fire,
- to increase the ambient concentration of O_2 in the compartment.

This oxygen availability assumption (Equation 3.6) is based mainly on the characteristics of the surrogate fuel which is taking part in the gas phase combustion. A sensitivity analysis of an influence of surrogate fuel definition to heat release rate and temperature progresses was conducted.

Simulations with enough oxygen for combustion available and lacking the oxygen were considered based on t-squared fire curve assumption. The process of assessing the t-squared fire curve was followed as stated above. Then, all the parameters were preserved the same for all the simulation and the only input changed was fuel input which is being defined to REAC. All the used surrogate fuels with some of their characteristics are shown in tables below. More built-in fuels and their characteristic are given in table 15.1 of FDS User Guide [10].

Table 4: Fuel inputs used within REAC command.

| Fuel | Formula | Molecular Weight [g/mol] |
|-----------|-------------|--------------------------|
| Propane | C_3H_8 | 44.095 |
| Butane | C_4H_{10} | 58.122 |
| Hydrogen | H_2 | 2.015 |
| Acetylene | C_2H_2 | 26.037 |
| Methane | CH_4 | 16.042 |

As a representative simulation with sufficient oxygen available a compartment with window of 5 m width was considered. The progresses of calculated rates of heat release are plotted in Figure 40.

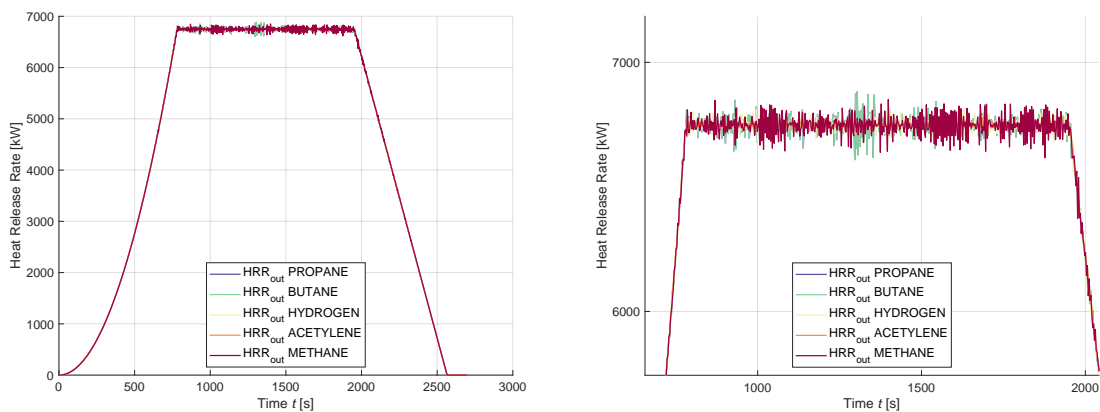


Figure 40: Comparison of output heat release rates for different fuel inputs assuming window width 5 m.

The heat release rates for all considered fuels follow the prescribed progress of t-squared fire curve and vary only within their horizontal plateau in little fluctuations. The overall progress is following

the t-squared fire (original progress is plotted in Figure 39).

Then a compartment with 1-m-wide window was simulated to examine the ventilation-controlled case. The prescribed heat release rate via t-squared fire is plotted in Figure 39) and the outcome rates of heat release are plotted in Figure 41.

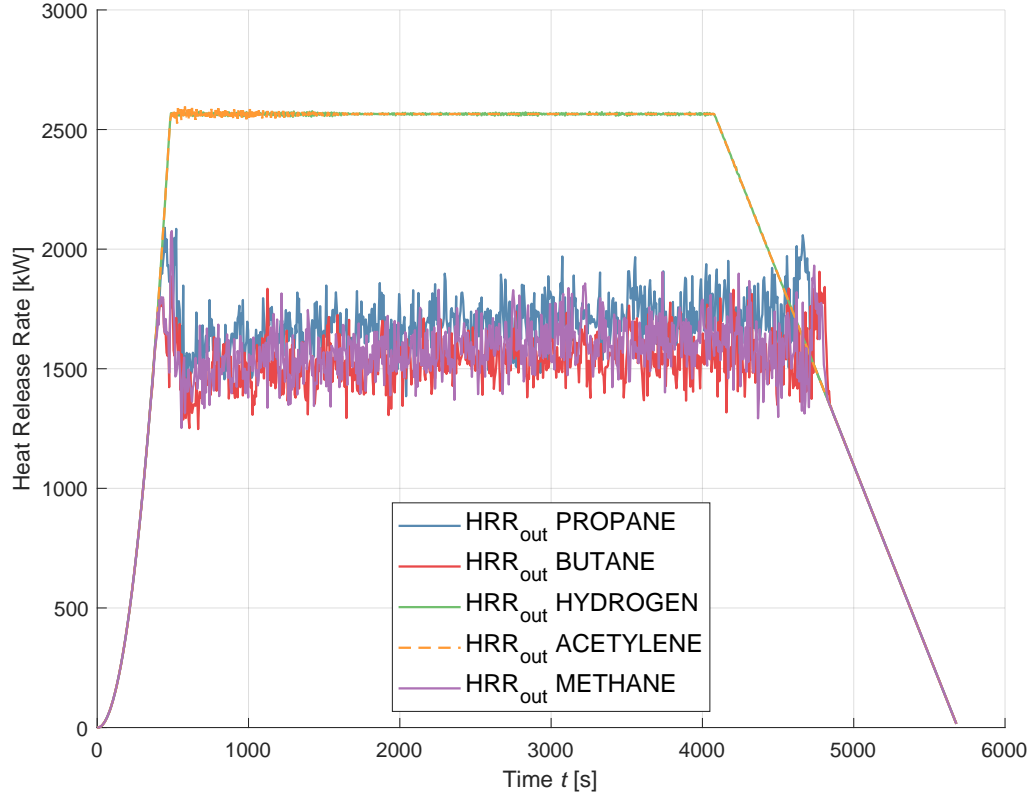


Figure 41: Output HRR progresses for different fuel inputs assuming window width 1 m.

A smoothing function⁵ in MATLAB [18] is used to for clearer representation of the results, which are then compared in Figure 42.

⁵Local regression using weighted linear least squares and a 2nd degree polynomial model.

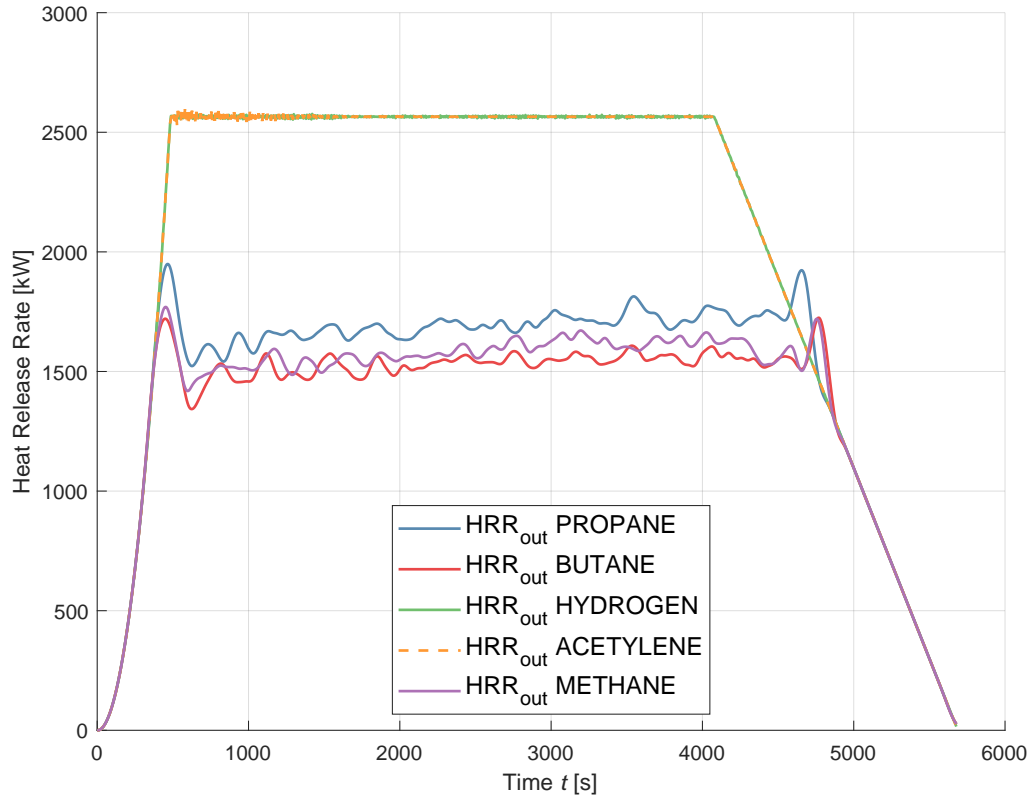


Figure 42: Smoothed output HRR progresses assuming different fuel inputs for window width 1 m.

The progress of calculated HRR for hydrogen and acetylene fuel follows the prescribed fire curve (Figure 39). Heat release rate progresses from simulations with propane and butane are reduced by 800–1000 kW⁶.

When taken proper look to the fuels' chemical characteristic and implemented extinction model assumptions:

The extinction model used for these particular simulation is model Extinction 2. It considers both the oxygen and the fuel content of a given grid cell at the beginning of a time step. If the potential rate of heat release from the reactants cannot raise the cell's temperature above the empirically determined critical flame temperature, combustion is suppressed. [9]

⁶These values of HRR can be for example reached by burning of lightly upholstered chairs within first 100–500 s of fire. See Figure 3-1.16 [6].

Table 5: Reaction's characteristics assuming different fuel inputs defined within REAC command.

| Fuel | Heat of Combustion [kJ kg ⁻¹] | Enthalpy of Formation [J kg ⁻¹] |
|-----------|---|---|
| Propane | 46,334 | $-2.37 \cdot 10^6$ |
| Butane | 45,720 | $-2.16 \cdot 10^6$ |
| Hydrogen | 119,960 | 0 |
| Acetylene | 48,278 | $8.76 \cdot 10^6$ |
| Methane | 50,010 | $-4.67 \cdot 10^6$ |

Table 5 includes enthalpy of formation for simulations each with different fuel defined in REAC namelist. The negative enthalpy of formation indicates that the amount of energy taken to break bonds is less than energy released when making new bonds. That state is referred to as exothermic and means, that the reaction produces heat. This applies for acetylene and hydrogen. The positive enthalpy of formation in contrast indicates that the amount of energy taken to break bonds is more than energy released when making new bonds and is called endothermic. That means the reaction requires heat. That applies for simulations with propane, butane and methane. [15]

So, in case of exothermic enthalpies of formation, it is assumed the energy released (calculated by Equation 3.6) raise the temperature of the cell above the critical flame temperature and the Extinction sub-model is not applied, as observed in Figure 42 for hydrogen and acetylene.

To support the fact, that extinction sub-model has been used is to calculate the HRR manually by equation

$$HRR_{calc} = \dot{m}_F''' \cdot \Delta H, \quad (4.2)$$

where

- \dot{m}_F''' is mass production rate of the fuel [kg s⁻¹],
- ΔH is heat of combustion of the fuel [kJ kg⁻¹].

If inequality $HRR_{calc} > HRR_{out}$ applies, there is unburned fuel leaving the compartment. The HRR curves calculated from the Equation 4.2 are compared to the HRR outcome from FDS in Figure 43.

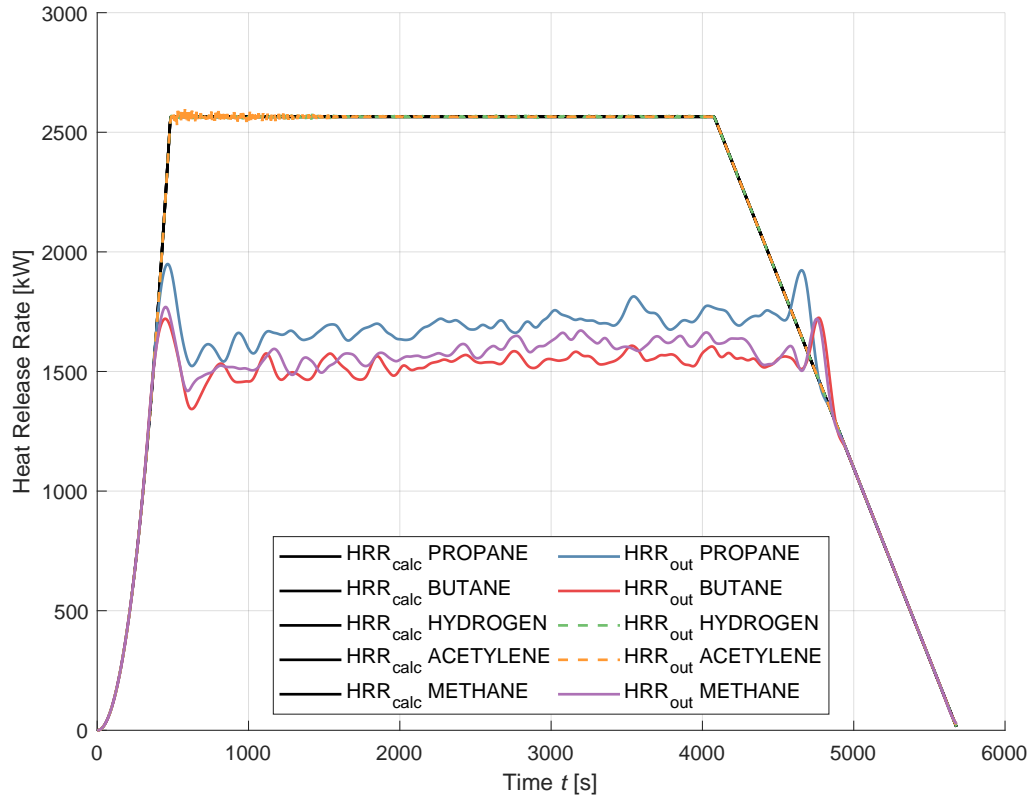


Figure 43: Comparison of HRR outcome and HRR calculated manually for different fuel inputs in simulation with window width $w = 1$ m.

The calculated HRR curves have the same progress for all considered fuels and have progress of the t-squared fire defined as an input. The progresses of outcome heat release rates from simulations with hydrogen and acetylene follows the progress as it is assumed sufficient energy to raise the cells' temperature above the empirically determined critical flame temperature, thus no unburned fuel is leaving the compartment.

The same simulation, which has been conducted with propane and is plotted in Figure 39, has been modelled with acetylene. The t-squared fire is considered to be unrestricted (for example as in simulation with 5-m-wide window) and is used as an input to simulation with 1-m-wide window. The progresses of HRR outcome of both propane and acetylene are plotted in Figure 44.

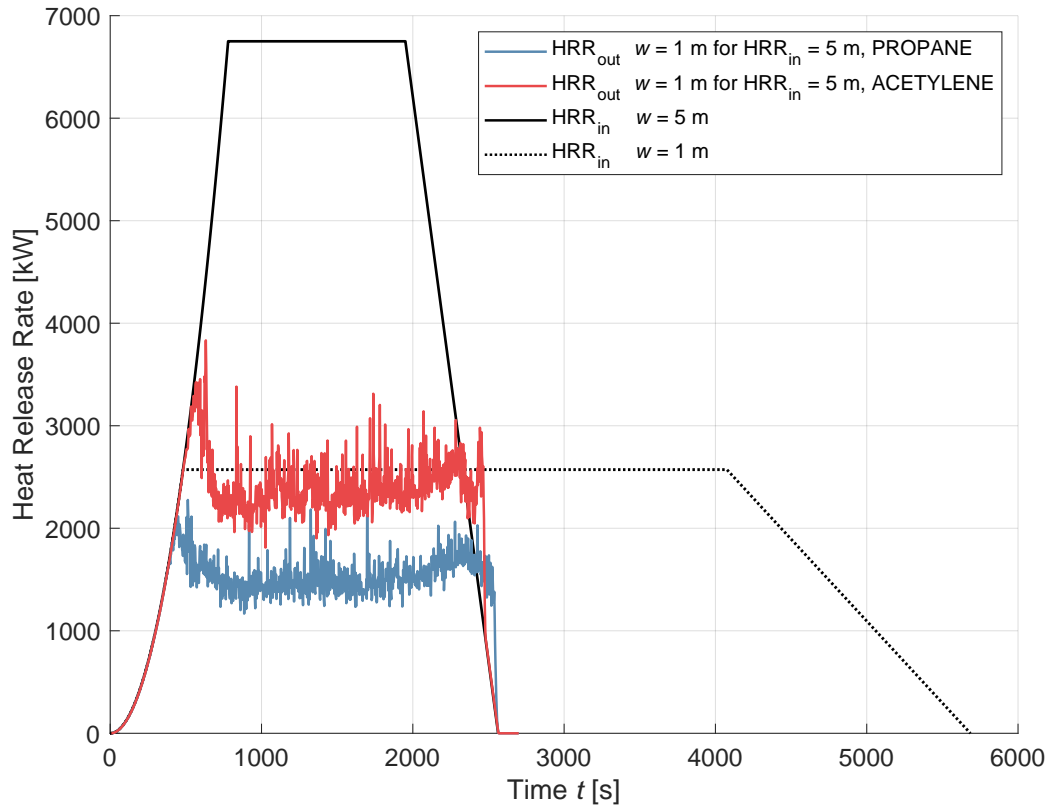


Figure 44: Demonstration of FDS inputs limitation due to insufficient oxygen availability. T-squared fire curves denoted as HRR_{in} for window widths $w = 1$ and $w = 5$ m are compared to HRR outcome from FDS simulation with 1-m-wide window with energy input for $w = 5$ m with propane and acetylene.

The progress of HRR outcome from simulation with acetylene is more likely to follow progress of the horizontal plateau of fire curve restricted by the simplified equation 2.2. However FDS is set to follow the prescribed t-squared fire curve HRR_{in} $w = 5$ m and does not maintain the released energy by prolonging the curve as it is done with the curve HRR_{in} $w = 1$ m.

It has been demonstrated that when inserting t-squared fire curve as an prescription of the rate of heat release, it depends not only on the size of the opening area and thus the oxygen availability, but also on the chemical characteristic of a fuel considered to take part in the combustion process. Taking into account the fact, that the fuel used as an input to the simulation should serve as a surrogate fuel to all the combustibles in the compartment, the author suggest the most proper step-by-step definition of the fire in FDS simulation:

1. Define the release of gaseous products by t-squared fire curve with its maximum progress, unrestricted,
2. define the fuel, which substitutes the combustibles present in the compartment and takes place in the process of combustion, based on a real knowledge about the the chemical characteristics

of the combustibles in the compartment,

3. calculate or make an assumption of mean maximum heat release rate from the restricted horizontal plateau by the software,
4. adjust m from equation 2.2. m is the combustion factor which represents the efficiency of combustion, varying between 1 for complete combustion to 0 for combustion fully inhibited. When derived and equation 4.3 is obtained:

$$m = \frac{Q_{max}}{0.1 \cdot Hu \cdot A_v \cdot \sqrt{h_{eq}}}, \quad (4.3)$$

where Q_{max} is substituted by mean maximum HRR determined in previous step,

5. determine new t-squared fire progress as in the first step, with adjusted m ,
6. define the rate of heat release by a prescription of the adjusted curve.

4.5.5 Temperature Outcome

The temperature in the compartment was taken as an average from 79 temperature measures by thermocouples placed regularly throughout the compartment as shown in Figure 45.

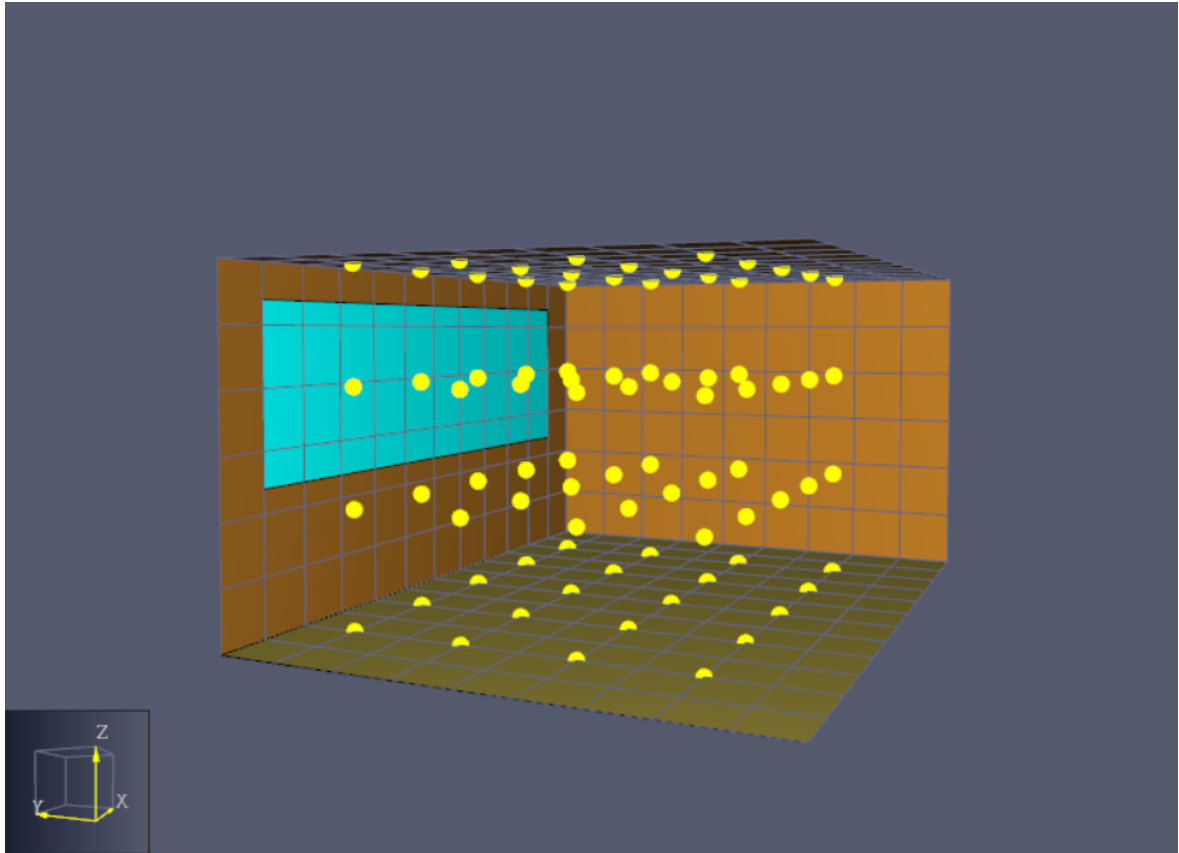


Figure 45: Simulated compartment with thermocouples. Screenshot by author.

First and assessment of an influence of ventilation to temperature progress was done. A comparison of temperatures from simulation with different window widths and corresponding energy release to the window width, included in Figure 46. The fuel defined in REAC to substitute the fuel present in the compartment was set to be propane.

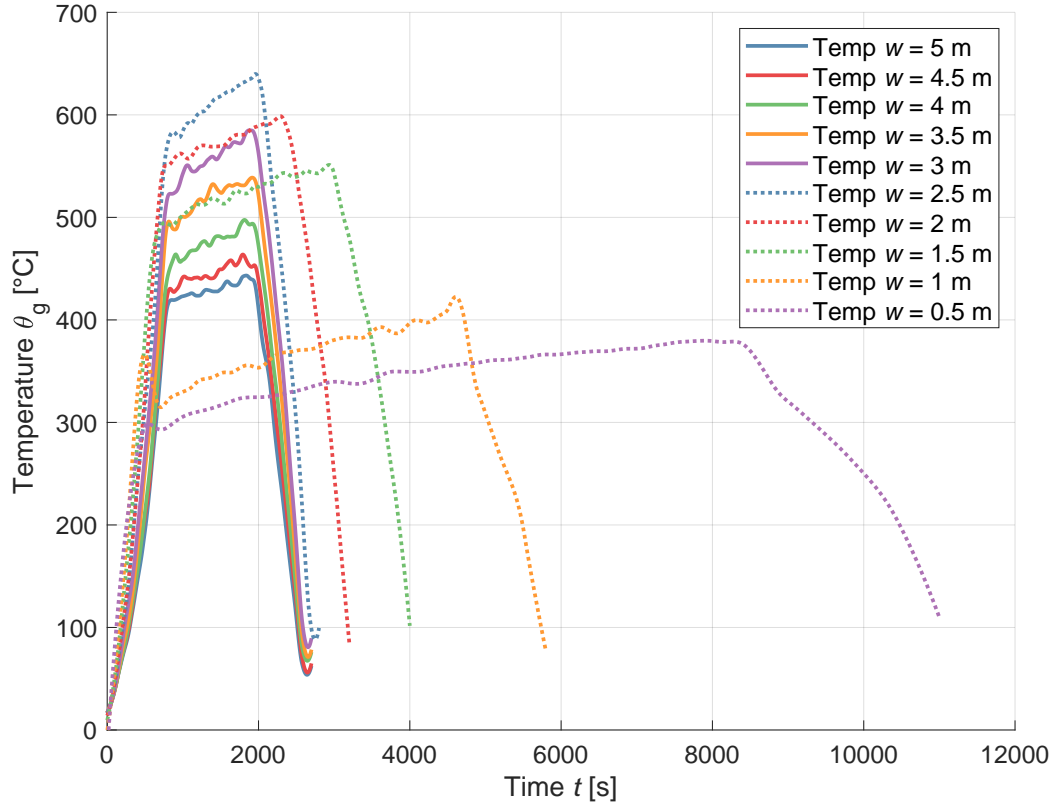


Figure 46: Smoothed average temperature progresses from FDS simulation for different opening areas with propane as a surrogate fuel.

A more detailed look not only to pyrolysis process definition, but also to gaseous fuel combustion process specification is included next. As stated in the theoretical part of this thesis, the fuel specified in simulation as a surrogate fuel, should be the as much corresponding to the present combustibles in compartment as possible.

An assessment of the influence of different fuels specifications in simulation to temperature outcome was conducted. Five built-in fuels were considered: propane, butane, hydrogen, acetylene and methane. Their chemical characteristics are given in Table 4.

Two basic cases are considered. Fuel-controlled simulation, with a window width of 5 m. The simulation with 1-m-wide window applies for ventilation-controlled case. The burning regime is assessed on the basis of simplified assumption given by Eurocode [8] and stated earlier in this thesis (Equation 2.2. The outcomes has been smoothened by a function in MATLAB [18] code to be able to represent

the results clearer.

The average temperature progresses from fuel-controlled simulation of 5-m-wide window for different surrogate fuel inputs are plotted in Figure 47.

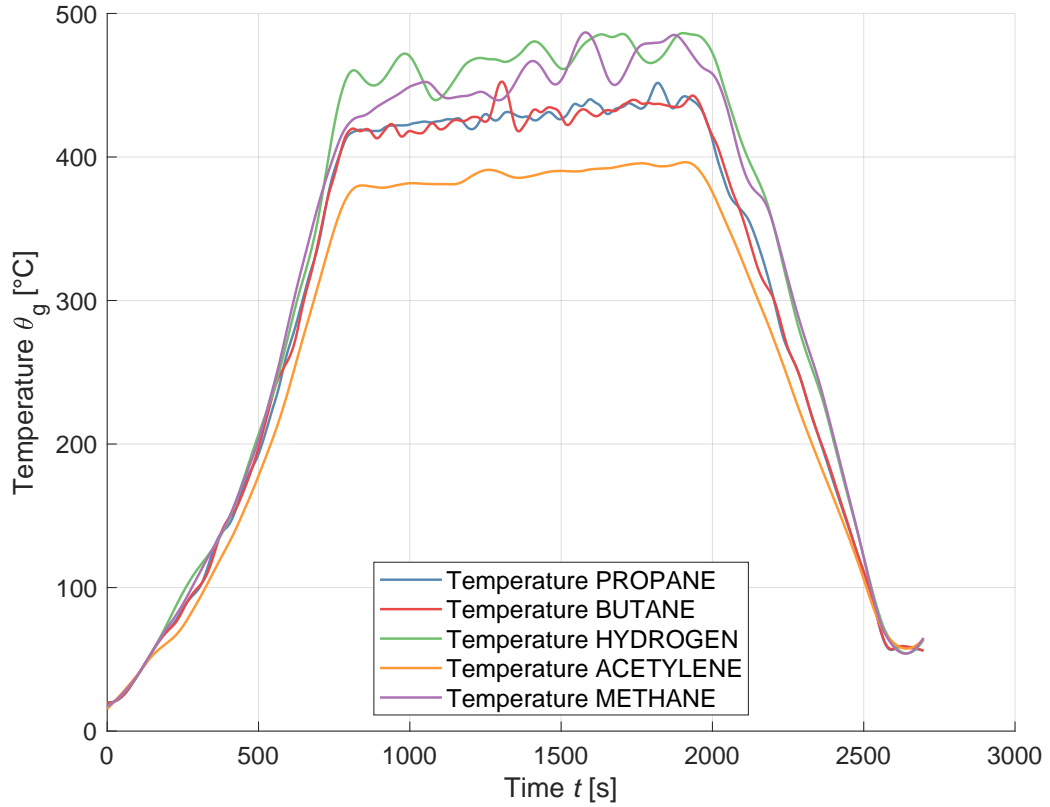


Figure 47: Smoothed average temperature progresses from FDS fuel-controlled simulations, each with different surrogate fuel definition.

The maximum peaks of simulation with hydrogen and methane are reaching values located slightly under the 500 °C with the biggest fluctuations. The medium progresses both in terms of temperature results and fluctuations are observed for propane and butane. The minimum reached temperature and the smoothest fluctuations are observed in simulation with acetylene.

The temperature outcome from simulations with different surrogate fuel inputs for ventilation-controlled energy, with window width of 1 m is plotted in Figure 49.

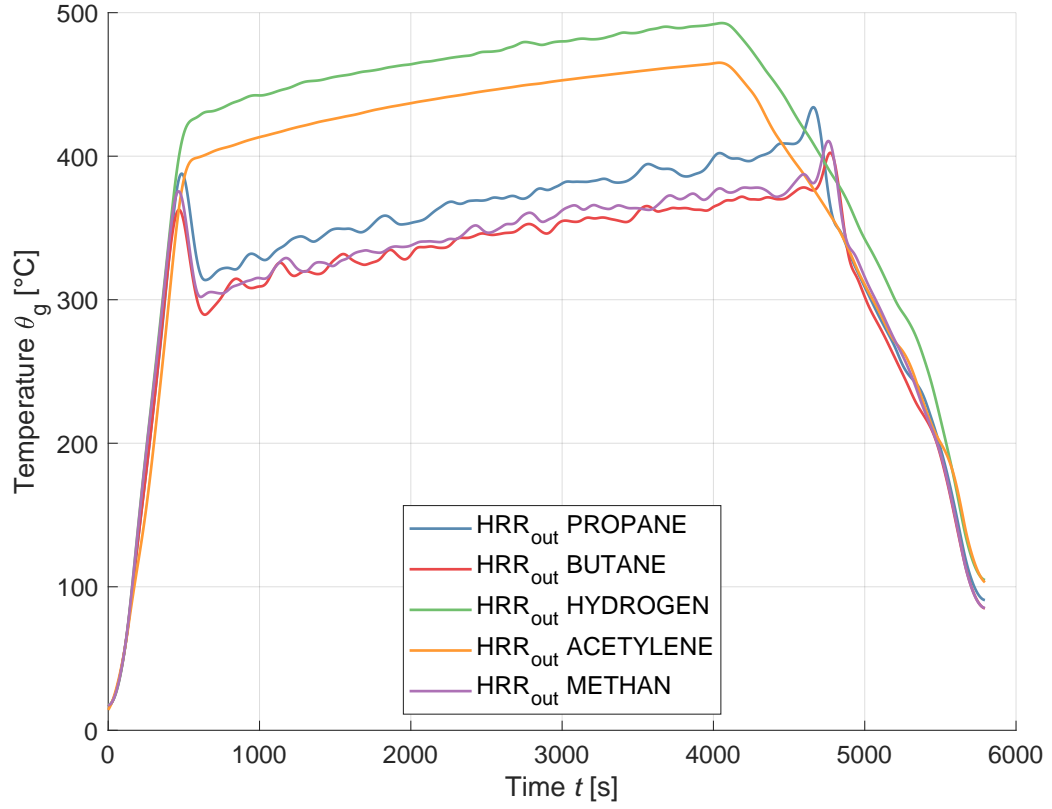


Figure 48: Smoothed average temperature progresses from FDS ventilation-controlled simulations, each with different surrogate fuel definition.

The fluctuations are observed in the temperature progresses from simulation with propane, butane and methane. The temperatures from simulations with hydrogen and acetylene are rather without any fluctuations. The order of the temperature progresses is linked to the order of the heat release rate progresses.

To assess whether this applies for the fuel-controlled case, the temperature progresses for both cases are plotted in Figure 49.

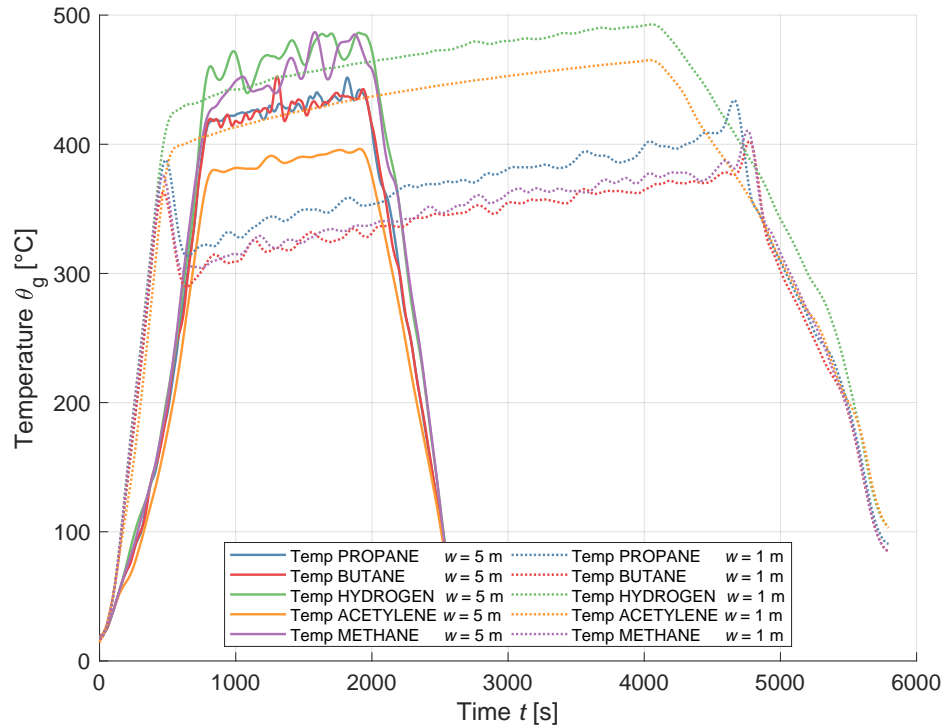


Figure 49: Smoothed average temperature progresses from FDS both fuel-controlled and ventilation-controlled simulations, with different surrogate fuel definition.

The order of the temperature progresses with different fuels involved for simulation with and without sufficient availability of oxygen does not correspond between the burning regimes. This is observed due to FDS assumption of ventilation influence and its implemented extinction sub-model.

As demonstrated, the performance of CFD model depends closely on a proper description of the physics and chemistry directing the processes running the combustion in combination with appropriate initial and boundary conditions. Two fundamental elements play a major role in a appropriate simulation assessment - the first is the description of the fire science and the second is the concerning establishment of a proper numerical solution. A checklist of some of the important considerations regarding the problem set-up and the outcome examination are given in chapter 3 of SFPE Handbook [6].

4.6 Discussion about Fire Models with Respect to Structural Fire Design

The temperature outcome from analysed fire models are plotted and compared in Figures 50 and 51, based on their burning regime determined by the parametric fire curve. The surrogate fuel was chosen to be propane, based on the suggestion stated in [28].

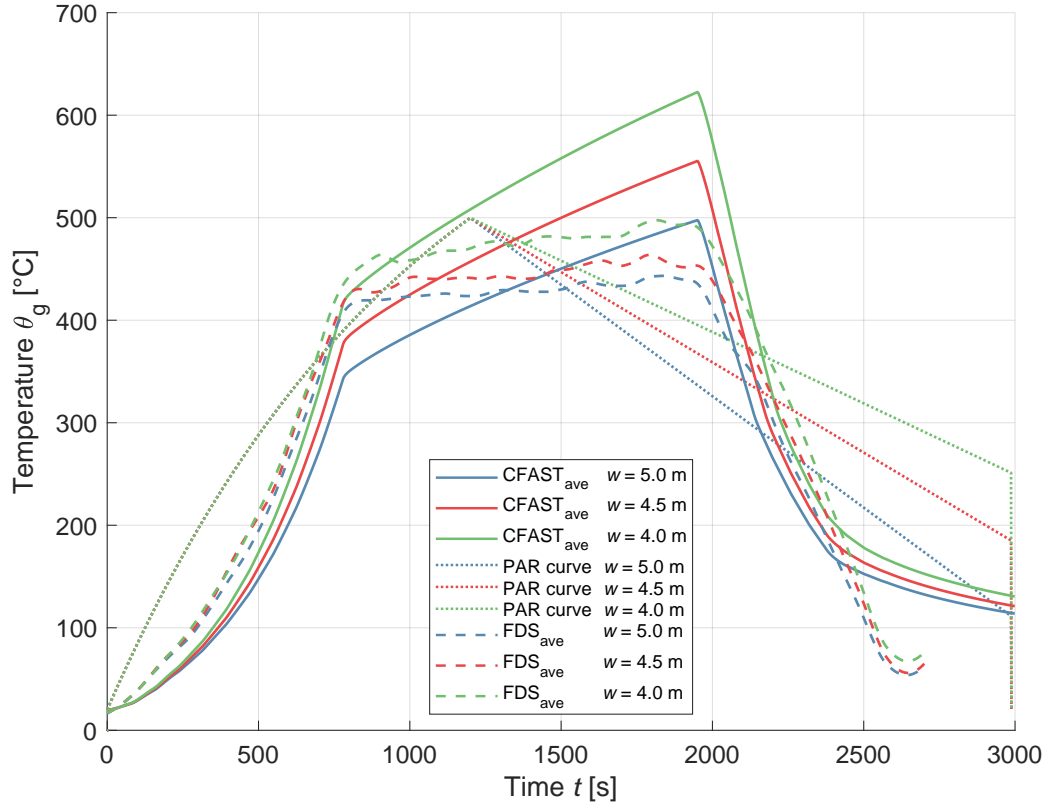


Figure 50: Final comparison of temperature progresses determined using the parametric fire curve, the zone model and the computational fluid dynamics model assuming window widths $<4 : 0.5 : 5>$ m.

The progresses do not vary rapidly. The highest values of temperature are reached by zone model. Even though the same energy input is used for both zone model CFAST and FDS, the temperature progresses vary. Temperatures from FDS are more alike to the t-squared curve input unlike the results from CFAST which have rather rising tendency.

The ventilation-controlled cases are included below.

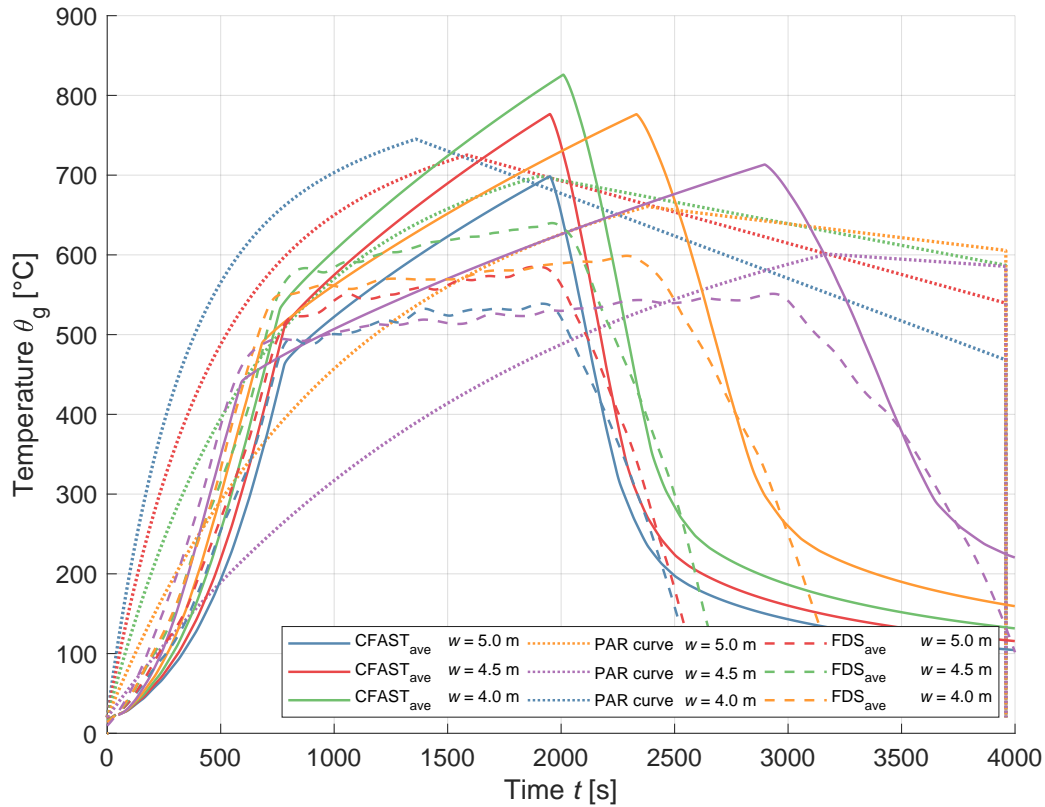


Figure 51: Final comparison of temperature progresses determined using parametric fire curve, zone model and computational fluid dynamics model assuming window widths $<0.5 : 0.5 : 3.5>$ m.

As in the case of fuel-controlled simulations, it is observed that the temperature progresses do not vary rapidly between different models as assumed formerly. The lowest temperature and in comparison to the CFAST progress, more consistent following of the prescribed t-squared curve is seen in the FDS temperature outcome. On the contrary, CFAST temperature outputs reach the highest values of maximum temperature which do not differ from the reached maximums by the parametric fire curve. As for the cooling part, the duration of the decay phase is the longest for the case of the parametric fire curve.

The accuracy and appropriateness of the models should be assessed regarding to a specific structural fire design analysis. Not only the fire model assumption but also the type of the input data must be assessed thoroughly based on the type and location of the structural element.

The purpose of averaging the temperature outcome served solely for the purposes of this thesis. Particularly mentioning the process of making an average temperature from two separate layers' temperature in zone model CFAST, even though the average was weighted, with the zone layers' height as the weight. The next averaged value was obtained as the arithmetic average from 79 thermocouples evenly distributes in CFD model. The purpose was to emphasize the size of the influence of little variations within the input data to the overall outcome.

While analysing specific structural element, it is essential to analyse its surrounding ambient and use the temperature or heat flux in the close region depending on the type of analysis and fire model.

In [3] an assessment of fire resistance of concrete structural members based on different fire models is conducted. Two conclusions are included. The first conclusion states that the numerical analysis of the structural element can be employed in connection with different fire models. The second conclusion demonstrated was that the fire resistance prediction of the structure element is strongly influenced by the type of the fire model directing the temperature progress analysis.

5. Discussion

Mentioning legislative system of the Czech Republic, according to Act no. 133/1985 Sb. § 99, there are two possible ways to approach fire safety design. The first one and most widely used is a standardised approach. For a majority of buildings and constructions this approach is sufficient. However, for assessing the fire threat and its possible outcomes more sophisticated approach can be used. As stated in Act no. 133/1985 Sb., it is possible to introduce performance based fire protection design.

Nevertheless it is essential to raise a query, when this approach is needed to be utilized as the performance based fire protection design is usually costly, both financially and from a time consumption point of view. Due to this fact mainly, when possible, a normative approach is being used. The performance based design is used for more complex construction where standards can not be applied or when the limits stated within the standards are too restrictive.

In that case the performance based design is conducted to determine the potential fire outcomes and its influence to the structures. Depending closely on type of analysis, the most appropriate fire model should be introduced. For every fire model concept there are often software available to conduct the analysis in. The assumption should be based on a proper knowledge of the fire engineer about the model restrictions and limitations.

The fire models, however, should be thought as of tool more than a software, which miraculously change the input data to desired output data. A thorough assessment of appropriateness of input data and the outcomes from the fire model needs to be conducted. That is connected not only with the experience but also with the knowledge of the fire model solving concept and mathematical apparatus implemented in the particular software, which is being used for the analysis.

Thus, not only from a legislation point of view, but also from the point of view of conscience of the fire engineer, a proper examination needs to precede the analysis itself to conduct an adequate and realistic piece of work.

A round-robin study [13] was conducted, to assess the variation in results due to user effect in simulation with FDS. It shows variations between users and their specification of input data, type of output data and the way of measuring them. However not only relatively large differences within the definition of the issue were observed, some of the participating users also made mistakes in the definition of fire. The paper states, that when the rate of heat release and wall boundary conditions were defined correctly, a sufficient prediction of temperature progresses could have been made.

The study demonstrates that when given a certain fire model and input data, assumption of each user may vary. As the personal input cannot be neglected, the overall knowledge of the model concept, mathematical apparatus used and simplifying assumption made (for example to simplify the calculations to reduce the calculating time required). As in the case of FDS, it does not only provide the

user with user guide [10], but also technical reference guide is available to provide information about physical and chemical laws directing the calculation and their way of implementation in the model itself. It has been demonstrated that despite of the sophistication of the implemented sub-models and relations, it is imperative to understand the processes running the fire model.

With performance-based design approach to analysis of a building structure, the understanding of fire characteristics is required for the overall performance of the analysis of the structure. It is primarily essential to assess the selection of fire model based on desired output data accuracy. At the same time it is impossible to assume that with *any* input data it is possible to obtain *any* required outputs, so a convenient determination preceding the analysis itself should be taken up. A knowledge about the concept, both physical and mathematical, of the fire model should be inevitable. That could play a major role in the fire outcome analysis and following structural fire design.

6. Conclusion

This thesis examines the extent of the influence of ventilation to energy release progress and temperature development in a compartment assuming three different fire models. The diploma thesis is divided into two main parts. The *first* part describes different fire phases and influencing factors playing a major role at enclosure fire development. Later, it examines the possibilities of fire definition and modelling and its fundamental functioning particularly focused on fire models used in the empirical part. The parametric fire curve from Eurocode 1991-1-2, zone model based software CFAST, and the computational fluid dynamics based model FDS are thoroughly discussed and used for the following analysis.

In the *second* – empirical part of the thesis a sensitivity analysis examining the influence of ventilation to energy release and temperature progress is conducted, assuming the three different models. A single, rather small compartment is modelled. Geometry and surrounding constructions' material characteristics are assumed to remain equal throughout the simulations. The assessment consists of deviating sizes of an opening area, and examines the variations of energy and temperature development as a consequence of the different models' assumptions. Subsequently, a sensitivity analysis in Fire Dynamics Simulator is conducted to assess the influence of different chemical formula, which substitutes the present combustibles in the compartment, to the heat release rate and the temperature development. The burning process is prescribed with the t-squared fire curve defined by Eurocode 1991-1-2 dependent on the size of the opening area, which changes. The results obtained from the parametric curve, the zone model, and the computational fluid dynamics model are compared and discussed in the later section. It is emphasized that the fire model assumption should be assessed based on the structural fire design analysis. An appeal on conscience of all fire engineers regarding a proper assessment of available input data related to desired data is included in the discussion section.

It is emphasized, that although a sophisticated fire model – which CFD without any doubts is – is introduced, it can not substitute the incompleteness and the inappropriateness of the input data. Thus, it is essential to understand the physics and mathematics directing the background calculations. Finally, before the ambient concentration of O_2 in FDS, computational fluid dynamics model using numerical analysis – which solves issues involving fluid flows – is changed, a determination of an appropriateness of such a solution should be reconsidered.

List of Figures

| | | |
|----|--|----|
| 1 | A graphic illustration of a difference between the process of pyrolysis and gas phase combustion. | 4 |
| 2 | Fire development stages with regards to temperature progress within the compartment. Reprinted from [6]. | 5 |
| 3 | An energy input defined by pyrolysis prescription over the compartment's floor. | 7 |
| 4 | An example of t-squared fire curve for a hotel room. | 8 |
| 5 | Illustration of t-squared fire progresses. Red colour illustrates fuel-controlled fire (with enough amount of oxygen), while the black color stands for ventilation-controlled curves whose horizontal plateau have been restricted by Equation 2.2. | 10 |
| 6 | Illustrative caption of emphasizing the influence of the size of the compartment's opening. | 11 |
| 7 | Distribution of flow income and discharge assumed by theoretical analysis of pressure difference when deriving the ventilation factor. h_F refers to the part of window, where only a discharge of the hot gases takes place. h_0 indicates the part, where the cold air enters the room. According to [14]. | 12 |
| 8 | Illustrative caption of emphasizing the influence of the geometry of compartment. | 13 |
| 9 | Illustrative caption of emphasizing the influence of the type, characteristics and width of the compartment's surrounding constructions. | 14 |
| 10 | Illustrative caption of emphasizing the influence of the size, type and location of the ignition source. | 14 |
| 11 | Spoiler illustration of a difference between fire models discussed below. It exemplify parametric fire curve model, zone model and field type model. | 15 |

| | | |
|----|---|----|
| 12 | Heat losses and gains during a fully developed compartment fire. The source of energy is \dot{q}_C , which is rate of heat release due to combustion. The energy losses are \dot{q}_L , which is rate of heat loss due to replacement of hot gases by cold, \dot{q}_W rate of heat loss through the walls, ceiling and floor and \dot{q}_R rate of heat loss by radiation through the openings. According to [7]. | 17 |
| 13 | Illustration of parametric curve progresses for the ventilation factor $O = <0.02; 0.2>$ with a 0.002 step. | 18 |
| 14 | Basic principle of zone model. According to [4]. | 19 |
| 15 | Illustration of a mesh in CFD model. | 21 |
| 16 | Grid cell. According to author's imagination. | 23 |
| 17 | Viability of combustion for an array of initial temperatures and oxygen concentrations. Reprinted from [10]. | 25 |
| 18 | Geometry of the analysed compartment. | 28 |
| 19 | Floor plan of analysed compartment with indicated dimensions. | 29 |
| 20 | Cross-section of analysed compartment with indicated dimensions. | 29 |
| 21 | Illustration of parametric curve progresses assuming window width $w = <1.5; 5>$ m with step of 0.5 m. | 31 |
| 22 | Parametric fire curve progress assuming window width 3.5 m. | 32 |
| 23 | Parametric fire curve progress assuming window width 4.0 m. | 32 |
| 24 | Defining a fire by t-squared curve in CFAST. | 33 |
| 25 | Comparison of t-squared fire curves assuming different window widths, used as HRR inputs for CFAST. | 34 |
| 26 | Comparison of input HRRs (t-squared fire curves) and HRR outputs. | 36 |
| 27 | Demonstration of CFAST inputs limitation due to insufficient oxygen availability. T-squared fire curves denoted as HRR_{in} for window widths 1 and 5 m are compared to HRR output from zone model based CFAST simulation with 1-m-wide window with energy input for 5 m. | 37 |
| 28 | Comparison of lower layer temperature progresses from CFAST and fuel-controlled parametric curves assuming window widths $<4.0, 4.5, 5.0>$ m. | 38 |
| 29 | Comparison of upper layer temperature progresses from CFAST and fuel-controlled parametric curves assuming window widths $<4.0, 4.5, 5.0>$ m. | 39 |

| | | |
|----|--|----|
| 30 | Comparison of lower layer temperature progresses from CFAST and ventilation-controlled parametric curves assuming window widths $\langle 1.5, 2.0, 2.5, 3.0, 3.5 \rangle$ m. | 40 |
| 31 | Comparison of temperature progresses from CFAST and ventilation-controlled parametric curves assuming window widths $\langle 1.5, 2.0, 2.5, 3.0, 3.5 \rangle$ m. | 41 |
| 32 | Smoke layer's lower surface height. | 42 |
| 33 | Comparison of mean average temperature progresses from CFAST and fuel-controlled parametric curves assuming window widths $\langle 4.0, 4.5, 5.0 \rangle$ m. | 43 |
| 34 | Comparison of mean average temperature progresses from CFAST and fuel-controlled parametric curves assuming window widths $\langle 1.5, 2.0, 2.5, 3.0, 3.5 \rangle$ m. | 44 |
| 35 | Fire simulation at its 1000th second when the fire is fully developed. Screenshot by author. | 45 |
| 36 | Compartment geometry with different opening areas. Screenshots by author. | 46 |
| 37 | T-squared fire curves progresses used as input rates of heat release for different window widths within FDS simulation. | 47 |
| 38 | Comparison of HRR inputs (t-squared fire curves) and output HRRs from FDS simulation assuming different opening areas. | 49 |
| 39 | Demonstration of FDS inputs limitation due to insufficient oxygen availability. T-squared fire curves denoted as HRR_{in} for window widths 1 and 5 m are compared to HRR output from FDS simulation with 1-m-wide window with energy input for 5 m. | 50 |
| 40 | Comparison of output heat release rates for different fuel inputs assuming window width 5 m. | 51 |
| 41 | Output HRR progresses for different fuel inputs assuming window width 1 m. | 52 |
| 42 | Smoothed output HRR progresses assuming different fuel inputs for window width 1 m. | 53 |
| 43 | Comparison of HRR outcome and HRR calculated manually for different fuel inputs in simulation with window width $w = 1$ m. | 55 |
| 44 | Demonstration of FDS inputs limitation due to insufficient oxygen availability. T-squared fire curves denoted as HRR_{in} for window widths $w = 1$ and $w = 5$ m are compared to HRR outcome from FDS simulation with 1-m-wide window with energy input for $w = 5$ m with propane and acetylene. | 56 |
| 45 | Simulated compartment with thermocouples. Screenshot by author. | 57 |
| 46 | Smoothed average temperature progresses from FDS simulation for different opening areas with propane as a surrogate fuel. | 58 |

| | | |
|----|--|----|
| 47 | Smoothed average temperature progresses from FDS fuel-controlled simulations, each with different surrogate fuel definition. | 59 |
| 48 | Smoothed average temperature progresses from FDS ventilation-controlled simulations, each with different surrogate fuel definition. | 60 |
| 49 | Smoothed average temperature progresses from FDS both fuel-controlled and ventilation-controlled simulations, with different surrogate fuel definition. | 61 |
| 50 | Final comparison of temperature progresses determined using the parametric fire curve, the zone model and the computational fluid dynamics model assuming window widths $<4 : 0.5 : 5>$ m. | 62 |
| 51 | Final comparison of temperature progresses determined using parametric fire curve, zone model and computational fluid dynamics model assuming window widths $<0.5 : 0.5 : 3.5>$ m. | 63 |

List of Tables

| | | |
|---|---|----|
| 1 | Window widths with corresponding value of maximum HRR | 30 |
| 2 | Comparison of burning regime assumptions using the parametric fire curve and the t-squared fire curve. | 35 |
| 3 | Window widths with corresponding value of maximum HRR and burning regime assumption according to Eurocode 1991-1-2. | 48 |
| 4 | Fuel inputs used within REAC command. | 51 |
| 5 | Reaction's characteristics assuming different fuel inputs defined within REAC command. | 54 |

Bibliography

- [1] National Fire Protection Association (NFPA) 2019. *National Fire Protection Association Handbooks*. URL: <https://www.nfpa.org/Codes-and-Standards/All-Codes-and-Standards/Handbooks>. (accessed: 21.04.2019).
- [2] S. Benkorichi. *S. Benkorichi: Fire Dynamics Simulator Mesh Size Calculator*. URL: https://www.sbenkorichi.com/cgi-bin/fds_mesh/index_mesh.py. (accessed: 12.11.2019).
- [3] M. Benýšek, R. Štefan, and J. Procházka. “Analysis of Fire Resistance of Concrete Structural Members Based on Different Fire Models: An Illustrative Example of the Slab Panel Assessment”. In: *25th Concrete Days 2018*. Vol. 292. Solid State Phenomena. Trans Tech Publications Ltd, July 2019, pp. 173–182. DOI: 10.4028/www.scientific.net/SSP.292.173.
- [4] *CFAST – Consolidated Fire and Smoke Transport (Version 7) Volume 1: Technical Reference Guide*.
- [5] U.S. Secretary of Commerce on behalf of the United States of America. *NIST Standard Reference Database Number 69*. URL: <https://webbook.nist.gov/chemistry/>. (accessed: 28.11.2018).
- [6] D. D. *SFPE Handbook of Fire Protection Engineering*. 2008. URL: <https://books.google.es/books?id=v0YzjwEACAAJ>.
- [7] D. Drysdale. *An Introduction to Fire Dynamics*. Wiley, 2011. ISBN: 9781119976103. URL: <https://books.google.es/books?id=8Au5oOMAdsoC>.
- [8] EN 1991-1-2. *Eurocode 1: Actions on structures – Part 1-2: General actions – Actions on structures exposed to fire*. CEN, 2002.
- [9] *Fire Dynamics Simulator Technical Reference Guide Volume 1: Mathematical Model*.
- [10] *Fire Dynamics Simulator User’s Guide*.
- [11] CFAST – Consolidated Model of Fire Growth and Smoke Transport. *version 7.3.0*. U.S. Department of Commerce: National Institute of Standards and Technology, 2019.
- [12] M.L. Janssens. *Introduction to Mathematical Fire Modeling*. CRC Press, 2000. ISBN: 9781482279009. URL: <https://books.google.es/books?id=8dcgCAAAQBAJ>.
- [13] N. Johansson and M. Ekholm. “Variation in Results Due to User Effects in a Simulation with FDS”. In: *Fire Technology* (Sept. 2017). DOI: 10.1007/s10694-017-0674-y.

-
- [14] B. Karlsson and J. Quintiere. *Enclosure Fire Dynamics*. Environmental & Energy Engineering. CRC Press, 1999. ISBN: 9781420050219. URL: <https://books.google.es/books?id=R8TZkODVNGgC>.
- [15] K.W. Kolasinski. *Physical Chemistry: How Chemistry Works*. Wiley, 2016. ISBN: 9781118751213. URL: <https://books.google.cz/books?id=5EsKDQAAQBAJ>.
- [16] J. Kučera. “Parametric Models of Fire for EN 1991-1-2:2021”. MA thesis. Czech Technical University in Prague, Jan. 2019.
- [17] R. Štefan M. Benýšek. *FMC - Fire Models Calculator*. URL: <http://people.fsv.cvut.cz/www/stefarad/software/fmc/fmc.cz.html>. (accessed: 03.10.2019).
- [18] MATLAB. *version 7.10.0 (R2010a)*. Natick, Massachusetts: The MathWorks Inc., 2010.
- [19] LLC MatWeb. *Material Property Data*. URL: <http://matweb.com/index.aspx>. (accessed: 29.11.2019).
- [20] J.G. Quintiere. *Fundamentals of fire phenomena*. John Wiley, 2006. ISBN: 9780470091135. URL: <https://books.google.es/books?id=otFSAAAAMAAJ>.
- [21] V. Šálek. “Thermal Characteristics of Solid Materials for Modelling the Spread of Fires”. MA thesis. Vojtech.Salek@vscht.cz: University of Chemistry and Technology Prague, May 2018.
- [22] FDS – Fire Dynamics Simulator. *version 6.7.1*. U.S. Department of Commerce: National Institute of Standards and Technology, 2019.
- [23] Česká agentura pro standardizaci. *CSN Online*. URL: <http://www.agentura-cas.cz/csn-online>. (accessed: 27.11.2019).
- [24] International Organization for Standardization. *International Organization for Standardization*. URL: <https://www.iso.org/home.html>. (accessed: 01.11.2019).
- [25] National Institute of Standards and Technology. *CFAST, Consolidated Fire and Smoke Transport*. URL: <https://pages.nist.gov/cfast/index.html>. (accessed: 05.04.2019).
- [26] National Institute of Standards and Technology. *FDS and Smokeview Discussions*. URL: <https://groups.google.com/forum/#!msg/fds-smv/8fWEroF8cio/7KL0tFP1-j0J>. (accessed: 10.10.2019).
- [27] National Institute of Standards and Technology. *FDS-SMV, Fire Dynamics Simulator and Smokeview*. URL: <https://pages.nist.gov/fds/index.html>. (accessed: 01.04.2019).
- [28] F. Wald et al. *Modelování dynamiky požáru v budovách*. České vysoké učení technické v Praze, 2017. ISBN: 9788001056332. URL: <https://books.google.cz/books?id=6MdfswEACAAJ>.